

# Quantum circuit compilation and hybrid computation using Pauli-based computation

F.C.R. Peres<sup>1,2</sup> and Ernesto F. Galvão<sup>1,3</sup>

<sup>1</sup>International Iberian Nanotechnology Laboratory (INL), Av. Mestre José Veiga, 4715-330 Braga, Portugal

<sup>2</sup>Departamento de Física e Astronomia, Faculdade de Ciências, Universidade do Porto, rua do Campo Alegre s/n, 4169-007 Porto, Portugal

<sup>3</sup>Instituto de Física, Universidade Federal Fluminense, Avenida General Milton Tavares de Souza s/n, Niterói, Rio de Janeiro 24210-340, Brazil

Pauli-based computation (PBC) is driven by a sequence of adaptively chosen, non-destructive measurements of Pauli observables. Any quantum circuit written in terms of the Clifford+ $T$  gate set and having  $t$   $T$  gates can be compiled into a PBC on  $t$  qubits. Here we propose practical ways of implementing PBC as adaptive quantum circuits, and provide code to do the required classical side-processing. Our first scheme reduces the number of quantum gates to  $O(t^2)$  (from a previous  $O(t^3/\log t)$  scaling) at the cost of one extra auxiliary qubit, with a possible reduction of the depth to  $O(t \log t)$ , at the cost of  $t$  additional auxiliary qubits (second scheme). We compile examples of random and hidden-shift quantum circuits into adaptive PBC circuits. We also simulate hybrid quantum computation, where a classical computer effectively extends the working memory of a small quantum computer by  $k$  virtual qubits, at a cost exponential in  $k$ . Our results demonstrate the practical advantage of PBC techniques for circuit compilation and hybrid computation.

## 1 Introduction

Quantum computers promise to solve some computational tasks much faster than their classical counterparts. Such tasks include integer factoring [1], dynamical quantum simulation [2], solving systems of linear equations [3], and certain problems in graph, group and knot theory [4]. These algorithms demonstrate how large-scale, error-corrected quantum computers are expected to unlock several practical applications. However, the currently available devices - dubbed NISQ, an acronym coined by John Preskill standing for noisy intermediate-scale quantum [5] - have several limitations such as a limited number of qubits and qubit connectivity, and a considerable amount of coherent and incoherent errors.

While some impressive results have recently been demonstrated, with quantum computational advantage being achieved for non-trivial (albeit contrived) mathematical tasks [6, 7, 8], the lim-

itations of available devices preclude any serious practical implementation of the promising aforementioned algorithms. Therefore, and since fault-tolerant quantum computation might still be decades away, it makes sense to ask ourselves how we can best exploit the currently available NISQ technology to reach computational advantage for practical applications in the near term.

Due to the constraints of such devices, it is clear that any reasonable implementation must make use of small qubit counts and shallow circuits. Such requirements can be achieved by developing smart schemes wherein a classical computer and a small quantum processing unit (QPU) are combined to make the best use of the limited quantum resources. Some key results are hybrid quantum-classical algorithms for ground-state energy estimation of a quantum Hamiltonian using the variational quantum eigensolver algorithm [9], speeding up the solution to 3-satisfiability problems [10], and Bayesian inference using large data sets [11].

F.C.R. Peres: [filipa.peres@inl.int](mailto:filipa.peres@inl.int)

In line with this idea of reducing quantum resources, here we explore Pauli-based computation (PBC) [12], a model that uses a sequence of adaptively chosen, non-destructive measurements of Pauli observables to do universal quantum computation. We explore PBC as a compilation tool that can be used to trade (affordable) classical computation for quantum computation, but also as a natural framework to formulate a hybrid computation set-up wherein a classical (super)computer and a small quantum computer can be used to emulate a larger quantum machine.

More specifically, here we focus on the task of using PBC to compile large  $n$ -qubit Clifford+ $T$  quantum circuits, with  $t$   $T$  gates, into (often) less resource-demanding adaptive circuits that can be run on quantum hardware, using control and side-processing of a classical computer [12]. We start by presenting two different theoretical schemes for translating the sequence of non-destructive measurements of pairwise commuting  $t$ -qubit Pauli operators of a standard PBC back into the quantum circuit model in an efficient and practical way. Using the first of these schemes, the PBC can be carried out with  $O(t^2)$  gates and depth, while the second scheme requires a gate count of the same order but has a reduced circuit depth of  $O(t \log t)$ . These results improve upon the proposal found in [13] which is not only slightly more involved but also requires a number of gates that scales like  $O(t^3/\log t)$ . Besides these theoretical contributions, we also developed Python code to implement the efficient PBC circuit compilation we have just described. This code is available at <https://github.com/fcrperes/CompHybPBC> and can be used to perform two distinct tasks. In both tasks, we use *PBC compilation* to provide us with equivalent PBC circuits which often have lower depth and/or gate counts, and, under certain conditions, a smaller number of qubits than the corresponding circuit input to the code. The first task that can be performed is that of weak simulation of the original circuit. The second task consists of carrying out approximate strong simulation while simultaneously reducing the number of qubits required, by simulating some of them classically; we call these *virtual qubits* and this particular task *hybrid PBC*, following the terminology in [12].<sup>1</sup> This second task can be phrased

<sup>1</sup>Here, it is important to note that the first task - that

in a slightly different (albeit equivalent) manner as a way of using a classical computer to extend the number of qubits available to the QPU by  $k$  virtual qubits, with a cost exponential in  $k$ .

We expect this work to be relevant both in the near term and in the long term. Firstly, PBC compilation allows the efficient reduction of intermediate-sized quantum circuits into smaller instances that can be run on current or near-term quantum hardware. Secondly, this reduction of quantum resources (i.e. number of qubits, depth and/or gate counts) will remain relevant even when large-scale, fault-tolerant quantum computers become available. Finally, hybrid PBC might be of particular interest for supercomputing centers wherein the powerful, available classical machines can be used to extend the working memory of a small QPU.

This paper is organized as follows. We start by presenting a review of previous work (sec. 2). Then, in section 3, we discuss the theoretical contributions of our research. In section 4, we report a practical implementation of PBC via Python code and the corresponding numerical results achieved with it for a particular class of hidden-shift circuits and also for random quantum circuits. Finally, in section 5, we draw some conclusions and set out possible future lines of research.

## 2 Review of prior work

### 2.1 Classical simulation of quantum circuits

There are two distinct notions of classical simulation. Weak simulation refers to the ability to sample from the (exact) same output distribution as that of the quantum circuit we intend to simulate. On the other hand, strong simulation consists of (exactly) computing the probability of obtaining a specific computational outcome. Additionally, approximate versions of each of these tasks can

of *PBC compilation* together with the weak simulation of the original quantum circuit - is also a hybrid quantum/classical procedure in the sense that part of the computation is being carried out by the controlling classical computer. Even so, and in order to avoid possible confusion, the reader should keep in mind that here the term *hybrid PBC* is exclusively used to denote the second task explored in this paper, i.e. that of reducing the number of qubits needed by the quantum hardware, by simulating a certain number of *virtual qubits*.

also be considered. In approximate weak simulation, we sample from an output distribution that is  $\epsilon$ -close to the output distribution of the original circuit with respect to the  $\ell_1$ -norm. In approximate strong simulation, we estimate the probability of a certain outcome within a given error  $\epsilon$  that is either additive, multiplicative or relative, depending on the algorithm.<sup>2</sup> For more details on the different types of errors see [14].

The Gottesman-Knill theorem [15, 16] states that polynomial-sized, unitary Clifford circuits, i.e. circuits with only (i) stabilizer-state inputs, (ii) gates drawn from the Clifford set, and (iii) final measurements in the computational basis, are classically simulable in polynomial time (both in the weak and in the strong sense). On the other hand, by adding any non-Clifford single-qubit unitary to the available set of gates, universal quantum computation is unlocked. As stated in the introduction, quantum computers are strongly believed to be more powerful than classical computers. This means that, unlike unitary Clifford circuits, universal quantum circuits cannot be efficiently simulated by classical means.

Regardless, the ability to simulate increasingly larger universal quantum circuits is desirable because, on the one hand, it will allow us to validate initial fault-tolerant prototypes, and, on the other, it helps to establish the boundary between the tasks that can be classically computable and those that strictly require a quantum computer. Thus, there is a strong incentive to study ways of improving the exponential scaling of such classical simulators, making this a flourishing field of research.

Initial simulators had a runtime which scaled exponentially in the total number of qubits,  $n$ , of the quantum circuit. Since then, several different methods have been developed which have helped to improve this exponential factor. For example, using techniques based on tensor networks has given rise to simulators whose runtime scales exponentially not with the total number of qubits but rather with the tree width of the underlying graph of the circuit [17]; more recently, but still within this framework, Huang, Newman, and Szegedy have established a lower bound on the time complexity of strong simulation which

<sup>2</sup>In literature, the notion of *multiplicative* errors is often used in a broad sense that encompasses also the so-called *relative* errors.

goes as  $2^{n-o(n)}$  [18].

Another approach is to use quasi-probability methods. In this context, Pashayan, Wallman and Bartlett [19] proposed a classical strong simulation method for qudits whose runtime depends on a measure of the total amount of negativity in the quantum circuit. More recently, in [20], a phase-space algorithm for classical simulation was proposed which extends to quantum systems of any (finite) dimension. This algorithm allows to estimate the output probability of a computation performed by Clifford gates and Pauli measurements on negatively represented input states with a cost that is proportional to a robustness measure squared. This quantity has been proved to be smaller than or equal to the robustness of magic.

In the context of  $n$ -qubit Clifford circuits augmented by  $t$  non-Clifford gates, Aaronson and Gottesman [21] showed that such circuits can be classically simulated in a time that scales like  $O(2^{4t} \text{poly}(n))$ . Afterward, stabilizer-rank approaches [12, 22, 23, 24] have allowed to improve the exponential scaling even further to  $2^{\alpha t}$ , where  $\alpha < 1$ , both in the context of strong and weak simulation. At the moment of writing, the best known coefficients are  $\alpha = 0.228$  for weak simulation [22, 23] and  $\alpha = 0.3963$  for strong simulation [25].

Recently, [26] has combined the work done on stabilizer decompositions with tensor-network-based techniques to achieve enhanced strong classical simulation, allowing to successfully simulate random 50- and 100-qubit Pauli exponential circuits with up to 70  $T$  gates, as well as 50-qubit hidden-shift circuits with up to 1400  $T$  gates.

In this paper, instead of considering the task of classically simulating a given universal quantum circuit, we approach the problem from the perspective of using a less resource-demanding quantum circuit to simulate a circuit with larger qubit counts, depth and/or gate counts. Within this framework we focus on two different tasks.

We start by considering PBC compilation and the simulation of large circuits by circuits (often) requiring fewer quantum resources. Thus, the first obvious difference between this approach and the full classical simulation schemes described above is that, in our case, part of the computation is still executed on a quantum computer, while the other part consists of polynomial clas-

sical side-processing carried out by an assisting classical-control computer. As we will see, this procedure allows for the efficient (weak) simulation of the original circuit; the trade-off, however, is that the compiled quantum computation needs to be performed adaptively, i.e. interleaved with the classical processing.

Secondly, oftentimes, the task of weak simulation of universal quantum circuits is translated into the problem of computing certain probabilities or marginals, which are then used to carry out the sampling. This is true of tensor-network and phase-space algorithms, as well as some stabilizer-rank-based simulators (e.g. [12, 22]). In contrast, our scheme executes a weak simulation of the original circuit without requiring the reduction to a strong simulation task.

Finally, compared against the weak simulators based on stabilizer-rank techniques proposed in [22] and [23], which allow to approximately sample from the output distribution of the desired circuit, our method provides an *exact* weak simulation scheme.

The theoretical background behind this first scenario (which we call *Task 1*) is discussed in subsection 2.2 and sub-subsection 2.3.1.

Additionally, we also consider a second task (dubbed *Task 2*) wherein we reduce the demand on the number of qubits of the quantum hardware, by simulating some of the qubits classically (virtual qubits). The two main differences with respect to Task 1 are that (i) we now focus on the task of estimating the probability,  $p$ , that a given qubit yields the outcome 1, and (ii) a single estimate of  $p$  involves a decomposition into  $3^k$  different quantum circuits, where  $k$  is the chosen number of virtual qubits. Each of these circuits needs to be run for a total number of shots  $N$  which scales inverse polynomially with the precision desired for the estimate of  $p$ . We see that, in this case, and unlike Task 1, we need to run exponentially many circuits, so that this task is clearly *not* efficient. However, compared against the full strong classical simulation schemes described above, the use of a small QPU will (for many instances) prove advantageous as it lessens the demands on the classical machines. This will be discussed in more detail in sub-subsection 2.3.2.

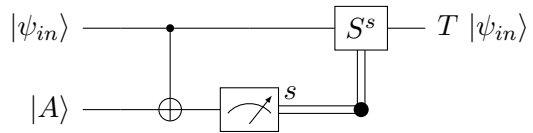


Figure 1: Implementation of the  $T$  gate via the well-known  $T$ -gadget.

## 2.2 The extended Gottesman-Knill theorem

We consider (universally general)  $n$ -qubit unitary Clifford+ $T$  quantum circuits with  $t$   $T$  gates and  $m$  final measurements in the computational basis. Here, the non-Clifford gate  $T$  is defined as  $T = \text{diag}(1, e^{i\pi/4})$ . It is well known [27, 28] that a  $T$  gate can be implemented via the  $T$ -gadget illustrated in Figure 1, so that the original unitary Clifford+ $T$  circuit  $\mathcal{U}$  is transformed into an adaptive Clifford circuit  $\mathcal{C}$  with input state  $|0\rangle^{\otimes n} |A\rangle^{\otimes t}$ ,  $t$  intermediate and  $m$  final measurements in the computational basis. Here, the state  $|A\rangle$  is the magic (i.e. non-stabilizer) state defined as  $|A\rangle = (|0\rangle + e^{i\pi/4} |1\rangle)/\sqrt{2}$ . These circuits are extremely alluring because they are written exclusively in terms of Clifford gates which can be realized fault-tolerantly using stabilizer codes [15, 16]. However, this implementation comes at the high practical cost of a larger number of logical qubits ( $n + t$  instead of  $n$ ). Additionally, it becomes necessary to devise protocols to purify imperfect magic states using Clifford gates only; for a review see [29, 30].

In [13], Yoganathan, Jozsa and Strelchuk used the Pauli-based model of quantum computation introduced in [12] (see subsec. 2.3) to prove that any such adaptive Clifford circuit  $\mathcal{C}$  can be reduced (using only a polynomial amount of classical resources) to an adaptive Clifford circuit  $\mathcal{C}'$  acting only on the magic state input  $|A\rangle^{\otimes t}$  and with at most  $t$  measurements in the computational basis. This result - dubbed by the authors the extended Gottesman-Knill theorem (Theorem 3.2 of [13]) - clearly provides a conceptual way of compiling general quantum circuits, minimizing the required quantum resources by trading in affordable and efficient (i.e. polynomial) classical processing.

As we will see below, in this context, PBC can be regarded as a useful intermediate step (or proof technique), as in this framework the reduction from  $(n + t)$  to  $t$  qubits happens simply and

naturally.

## 2.3 Pauli-based computation

### 2.3.1 Efficient circuit compilation

As mentioned in the last paragraph of the previous subsection, to understand how any universally general adaptive Clifford circuit acting on the input state  $|0\rangle^{\otimes n} |A\rangle^{\otimes t}$  can be reduced to a quantum computation on only  $t$  qubits, it is easier to consider Pauli-based computation (PBC). Following the terminology used in [12], we define a standard PBC  $\mathcal{Q}$  as follows:

- The input state is a product state of magic states:  $|A\rangle^{\otimes t}$ ;
- Operations are *non-destructive* measurements of independent and pairwise commuting Pauli operators,  $P_i$ , belonging to the Pauli group on  $t$  qubits,  $\mathcal{P}_t$ ;
- The result of the computation is obtained from the outcomes  $s_i$  of the Pauli measurements together with some interleaved (polynomial) classical processing.

This definition allows us to write the following theorem (adapted from [12]):

**Theorem 1** *Any (universally general)  $n$ -qubit Clifford+ $T$  circuit  $\mathcal{U}$  with  $t$   $T$  gates can be simulated by a (standard) PBC  $\mathcal{Q}$  on  $t$  qubits and  $\text{poly}(n, t)$  classical processing.*

Theorem 1 is an assertion of the universality of the Pauli-based model of quantum computation but, as we will see, can also be regarded as a statement on the compilation of quantum computations.

The proof of this theorem is quite straightforward. We start by transforming the unitary  $n$ -qubit Clifford+ $T$  quantum circuit into an  $(n+t)$ -qubit, adaptive Clifford circuit with input state  $|0\rangle^{\otimes n} |A\rangle^{\otimes t}$  and  $(t+m)$  measurements in the computational basis.

Next, we initialize a generalized PBC list with  $n$  dummy single-qubit  $Z$  operators acting on each of the main (stabilizer-state) qubits:

$$\text{(LIST)} : Z_1, Z_2, \dots, Z_n. \quad (1)$$

Following this, we take the single-qubit  $Z$  measurement of the first auxiliary qubit,  $Z_{a_1}$ , and

propagate it through all the unitaries to its left until it reaches the very beginning of the quantum circuit. Because the circuit is made up only of Clifford gates, this can be done efficiently [15, 16] and the result will always be a Pauli operator:  $Z_{a_1} \rightarrow P_{a_1} = U_{a_1}^\dagger Z_{a_1} U_{a_1}$ , where  $U_{a_1}$  denotes the part of the circuit to the left of the measurement of the first auxiliary qubit and  $P_{a_1} \in \mathcal{P}_{n+t}$ . Once we have this Pauli operator at the very beginning of the circuit, we proceed in the following manner:

1. Assess whether the current Pauli,  $P_{a_1}$ , commutes or anti-commutes with any of the dummy  $Z_i$  operators or with any previously measured and pairwise commuting Pauli operators. (Of course, for the first Pauli, none of the latter operators exist yet, but as they start to arise they need to be considered in this step.)
2. If the current Pauli anti-commutes with a certain Pauli operator  $Q$ , it is clear its quantum measurement, if performed, would yield the outcome 0 or 1 with equal probability. Thence, instead of carrying out an actual (quantum) measurement, we can use a classical computer with a random number generator to randomly draw the measurement outcome  $s_{a_1}$  from the uniform distribution  $f_U = \{0, 1\}$ . To ensure that the quantum system is transformed into the correct quantum state that would be obtained after the measurement of  $P_{a_1}$ , we add the Clifford operator  $V(\lambda, s_{a_1}) = ((-1)^\lambda Q + (-1)^{s_{a_1}} P_{a_1})/\sqrt{2}$  at the beginning of the quantum circuit (before all other unitary gates). Here,  $\lambda$  denotes the outcome of the previously measured Pauli operator  $Q$ . Being a Clifford unitary, subsequent Pauli operators will be propagated through  $V(\lambda, s_{a_1})$  easily and efficiently.
3. If, on the other hand, the current Pauli commutes with all previously measured Pauli operators (and dummy  $Z$  measurements) there are two possibilities:
  - (a) either it depends on previously measured operators, in which case its outcome  $s_{a_1}$  is fully determined by the outcome of those operators, and can be determined classically;

- (b) or it is independent of previously measured Pauli operators, in which case we need to perform the actual measurement of  $P_{a_1} = P'_{a_1} \otimes P''_{a_1}$ , where  $P'_{a_1} \in \mathcal{P}_n$  and  $P''_{a_1} \in \mathcal{P}_t$  denote the Pauli operators acting on the main (stabilizer-state) and auxiliary (magic-state) qubits, respectively. Note that  $P_{a_1}$  is necessarily trivial on the stabilizer-state qubits, i.e.  $P'_{a_1} = Z^{b_1} \otimes Z^{b_2} \otimes \dots \otimes Z^{b_n}$ , with  $b_i = \{0, 1\}$ . Therefore, it is clear that we can reduce the measurement of  $P_{a_1}$  on all  $n+t$  qubits to the measurement of  $P''_{a_1}$  on the  $t$ -qubit auxiliary quantum register.

After we have determined the appropriate outcome  $s_{a_1}$  for this first Pauli operator  $P_{a_1}$ , we store it and fix the next part of the adaptive Clifford circuit appropriately. Finally, the Pauli operator is added to the generalized PBC list and (if case 3.(b) happened) to the list of actually measured quantum operators. Then we carry out the procedure described above for each subsequent measurement in the quantum circuit (going first through the measurements of the auxiliary qubits and only afterward through the  $m$  measurements of the main qubits), until the outcome of all the Pauli operators in the generalized PBC has either been classically determined (cases 2. and 3.(a)) or actually measured in a given QPU (situation 3.(b)).

The actual outcome of the computation is the bit string  $\mathbf{s}$  made up from the  $m$  outcomes of the last  $m$  Pauli operators (regardless of whether those outcomes were established classically or through real quantum measurements).

The procedure described guarantees that the actual quantum computation corresponds to the measurement of at most  $t$  independent and pairwise commuting Pauli operators on the  $t$  qubits initially in the product state  $|A\rangle^{\otimes t}$ . Therefore, we are simulating the original circuit by a standard PBC on  $t$  qubits, together with some classical processing which takes time  $poly(n, t)$ . (For more detailed proofs of some of the claims made along the procedure described above see refs. [12] and [13].)

It is important to realize that the compiled computation (i.e. the standard PBC) is not always the same. That is, each time we want a single-shot sample from the output distribution

of the original unitary Clifford+ $T$  circuit, the entire procedure described above needs to be executed, yielding a sequence of Pauli measurements (and, therefore, a standard PBC) which might differ from shot to shot. Only in this way can we guarantee that we are sampling from the correct output distribution.

At this point, we would like to draw the reader's attention to the fact that the extended Gottesman-Knill theorem formulated in [13] and summarized in the previous subsection corresponds simply to translating this standard PBC back into the quantum circuit model. In [13], the authors present a theoretical and abstract way of doing so. According to their proposal, if the outcome of a certain Pauli  $P_1 \in \mathcal{P}_t$  needs to be determined via an actual non-destructive quantum measurement (case 3.(b) above), then this can be done via a unitary Clifford circuit  $U(P_1)$  which maps the measurement of that  $t$ -qubit Pauli operator to the measurement of a single qubit (e.g. measurement of  $Z_1$ ). Using this translation back into the quantum circuit model we get the outcome  $s_1$  for  $P_1$  and can proceed with the PBC procedure described above until we find the next Pauli that needs to be measured, at which point we need to perform another translation back into the circuit model by finding the unitary  $U(P_2)$  which maps this new Pauli  $P_2$  to the  $Z$  measurement of another qubit (e.g.  $Z_2$ ). The general idea is illustrated in Figure 2 for a PBC on 2 qubits.

In [31], the authors showed that any CNOT circuit of  $n$  qubits has an equivalent CNOT circuit with only  $O(n^2/\log n)$  gates. On the other hand, Theorem 8 of [21] states that "*any unitary stabilizer circuit has an equivalent canonical form*" consisting of a sequence of 11 rounds each of which is made up exclusively of either phase, Hadamard or CNOT gates. It is straightforward to see that each phase or Hadamard round requires only  $O(n)$  gates, while a CNOT segment can be written with  $O(n^2/\log n)$  gates (as per the result of [31] stated above). Returning to the proposal of [13] for the conversion from PBC back to the quantum circuit model, it is easy to understand that each unitary  $U(P_i)$  can be efficiently found and implemented via a quantum circuit with  $O(t^2/\log t)$  gates. Since the standard PBC has potentially  $t$  independent and pairwise commuting Pauli observables, the  $t$ -qubit adaptive Clifford circuit proposed in [13] and used to

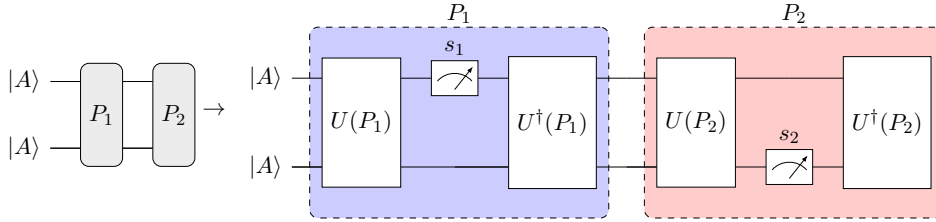


Figure 2: Implementation of an adaptive PBC via a sequence of adaptively-chosen Clifford circuits, using the approach proposed in [13]. Each colored box corresponds to the implementation of a single Pauli measurement, as described in the main text.

perform the computation has a total number of gates that scales like  $O(t^3/\log t)$ .

### 2.3.2 Hybrid Pauli-based computation

We have just explained how a certain input quantum circuit can be compiled into an adaptive PBC circuit with  $t$  qubits. From this explanation, it is clear that the compilation procedure is naturally interleaved with that of sampling from the output distribution of the original quantum circuit; in fact, the processes of compilation and weak simulation of the original quantum circuit using a QPU with (at least)  $t$  qubits together with (polynomial) classical processing are inseparable, and comprise what we name Task 1.

Besides this, ref. [12] discusses a related (yet distinct) task, which will now be explained; we call this Task 2. We start by restricting ourselves to the set of input Clifford+ $T$  quantum circuits with a single output measurement.<sup>3</sup> For such input circuits, we want to estimate the probability  $p$  of getting the outcome  $y = 1$ , with a relative error of (at most)  $\epsilon$ ; in other words, we want to make a strong simulation of the original input circuit. Assuming (just as before) access to a QPU with (at least)  $t$  qubits, this task can be achieved simply by carrying out the procedure outlined above a suitable number of times.

The questions posed and answered in [12] were the following: (i) can we perform the simulation task described above in a QPU with only  $t - k$  qubits?; and (ii) if so, what is the cost of simulating the  $k$  virtual qubits?

The first question can obviously be answered in the affirmative. As we have seen, any Clifford+ $T$  quantum circuit can be simulated by a standard PBC  $\mathcal{Q}$  on  $t$  qubits; now, if we only have  $t - k$

<sup>3</sup>This could be the case, for instance, of a circuit used to solve a decision problem.

qubits accessible in our quantum hardware, we can simply decompose the magic state  $|A\rangle\langle A|^{\otimes k}$  of the first  $k$  qubits into a stabilizer pseudomixture:

$$|A\rangle\langle A|^{\otimes k} = \sum_{i=1}^M \alpha_i |\psi_i\rangle\langle\psi_i|, \quad (2)$$

where the sum ranges over  $M$  pure  $k$ -qubit stabilizer states  $|\psi_i\rangle\langle\psi_i|$  and the coefficients  $\alpha_i$  are real numbers. Doing this gives us  $M$  generalized PBCs with input state:  $|\psi_i\rangle|A\rangle^{\otimes(t-k)}\langle\psi_i|\langle A|^{\otimes(t-k)}$ . Noting that any stabilizer state  $|\psi_i\rangle$  on  $k$  qubits can be obtained from the computational basis state  $|0\rangle^{\otimes k}$  by the application of a Clifford unitary  $U_i$ :  $|\psi_i\rangle = U_i|0\rangle^{\otimes k}$ , we realize that each of the  $M$  generalized PBCs can be transformed into a standard PBC on only  $(t-k)$  qubits, following the PBC compilation procedure described above.

As explained in [12], linearity implies that the probability  $p$  of getting the output 1 is simply given by:

$$p = p_{\mathcal{Q}} = \sum_i^M \alpha_i p_{\mathcal{Q}_i}.$$

Here,  $p_{\mathcal{Q}_i}$  denotes the probability that the output of the  $i$ -th standard PBC on  $(t-k)$  qubits yields 1.

Now, suppose that  $y_i$  is the output of a single shot of the (standard) PBC  $\mathcal{Q}_i$ . It is fairly obvious that  $\mathbb{E}(y_i)$  is an unbiased estimator of  $p_{\mathcal{Q}_i}$ , so that the expectation value  $\mathbb{E}(\xi)$  of the random variable  $\xi$  defined as:

$$\xi = \sum_i^M \alpha_i y_i \quad (3)$$

is an unbiased estimator of the desired probability  $p$  [12].

Next, we have to determine the number of samples,  $N$ , that need to be drawn from the output distribution of each PBC  $\mathcal{Q}_i$  in order to guarantee that  $p - \epsilon \leq \mathbb{E}(\xi) \leq p + \epsilon$ . Note that if we draw  $N$  values for each of the random variables  $y_i$ , this means we have  $N$  values for the random variable  $\xi$ . Thus, the error associated with the estimate of  $p$  is given by

$$\epsilon = \frac{1}{\sqrt{N}}\sigma(\xi) \leq \frac{1}{\sqrt{N}}\sqrt{\sum_i^M \alpha_i^2}.$$

If we want to estimate  $p$  with a confidence level of  $(1 - 1/c^2)$ , then Chebyshev's inequality determines that the corresponding confidence interval has the following lower and upper bounds:

$$\left[ \mathbb{E}(\xi) - \frac{c}{\sqrt{N}}\sqrt{\sum_i^M \alpha_i^2}, \mathbb{E}(\xi) + \frac{c}{\sqrt{N}}\sqrt{\sum_i^M \alpha_i^2} \right].$$

Finally, this tells us that if we want a precision  $\epsilon$ , the number of samples for each PBC needs to be:

$$N = \left\lceil \frac{c^2}{\epsilon^2} \sum_i^M \alpha_i^2 \right\rceil. \quad (4)$$

Obviously, since there are  $M$  different (standard) PBCs involved, the total number of shots is:  $\mathcal{N} = M \cdot N$ . The overall cost of this procedure is, therefore, directly connected to the value of  $M$ . For  $k = 1$  we can write explicitly:

$$|A\rangle \langle A| = \alpha_1 |+\rangle \langle +| + \alpha_2 |-\rangle \langle -| + \alpha_3 |+_i\rangle \langle +_i|,$$

where  $|\pm\rangle$  are the eigenvectors of the single-qubit Pauli operator  $X$  with eigenvalues  $\pm 1$ ,  $|+_i\rangle$  is the eigenvector of the single-qubit Pauli operator  $Y$  with eigenvalue  $+1$ , and the coefficients  $\alpha_i$  are

$$\alpha_1 = \frac{1}{2}, \quad \alpha_2 = \frac{1 - \sqrt{2}}{2}, \quad \text{and} \quad \alpha_3 = \frac{1}{\sqrt{2}}.$$

Hence, the trivial scaling of  $M$  with the number of virtual qubits  $k$  is:  $M = 3^k$ . We believe this scaling should be improvable although, to the best of our knowledge, no such proof can be found in current literature. However, it is clear that any improvements achieved for this scaling would have a direct impact on the performance of this hybrid computation.

The ideas described above are the essence of Theorem 3 of [12], stated here in an adapted form:

**Theorem 2** *Any (standard) PBC on  $t$  qubits can be simulated by  $2^{O(k)}$  (standard) PBCs on  $t - k$  qubits and a classical processing which takes time  $2^{O(k)} \text{poly}(t, k)$ .*

This Theorem highlights the second big merit of PBC, namely, that it allows a straightforward formulation of a hybrid computation wherein a classical (super)computer can be used to extend the number of qubits available to the QPU (albeit with an exponential overhead).

### 3 Optimized implementations of Pauli-based computation

In this section, inspired by quantum-error correction and syndrome measurement of Pauli operators, we introduce two alternative ways of implementing a standard PBC, i.e. of carrying out a sequence of  $t$  adaptive and non-destructive measurements of independent and pairwise commuting Pauli operators.

Our first approach requires the use of one auxiliary qubit whose measurement determines the outcome of the corresponding  $t$ -qubit Pauli operator. Consider that the observable to be measured (non-destructively) is  $P_i = \sigma_{i;1} \otimes \sigma_{i;2} \otimes \dots \otimes \sigma_{i;t}$ , where each  $\sigma_{i;j}$  denotes a single-qubit Pauli operator  $I, X, Y$ , or  $Z$ . Our method works by bringing in an auxiliary qubit in the state  $|+\rangle = H|0\rangle$ , and using it as the control qubit for the sequence of controlled- $\sigma_{i;j}$  operations each of which targets the corresponding main qubit  $j$ . After that sequence, a Hadamard gate is applied to the auxiliary qubit which is then measured in the computational basis. It is easy to show that, after this measurement, the main qubits are left in a state which is the  $(-1)^{s_i}$ -eigenstate of  $P_i$ , where  $s_i \in \{0, 1\}$  is the outcome of the measurement of the auxiliary qubit. This qubit can be reset and re-used to measure the next Pauli in the (adaptive) PBC sequence.<sup>4</sup> This proposal is illustrated in Figure 3 for the case of a simple 2-qubit PBC.

Clearly, the implementation of a  $t$ -qubit PBC using this scheme has a total depth of  $O(t^2)$  layers; additionally, the total number of gates also

<sup>4</sup>Note that resetting can be easily carried out by simply adding an  $X$  gate whenever necessary, i.e. whenever the outcome is 1.

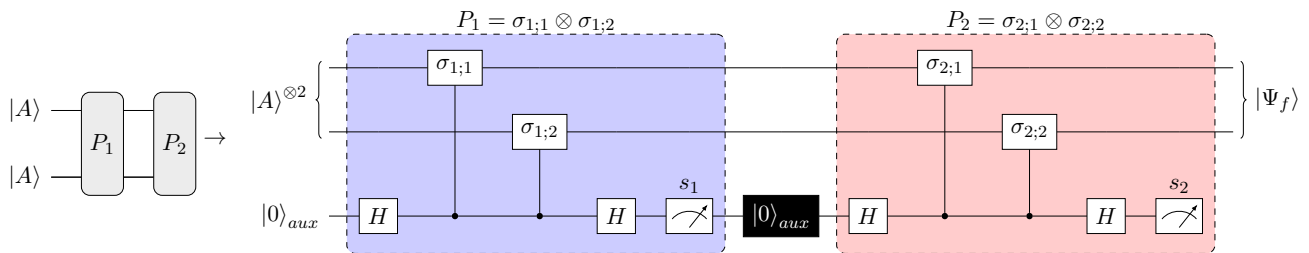


Figure 3: Our (first) proposal for carrying out the sequence of non-destructive measurements in the adaptive PBC obtained during the compilation process. Each colored box corresponds to the implementation of a single Pauli measurement, as described in the main text. The black box with label  $|0\rangle_{aux}$  indicates a re-setting of the auxiliary qubit in state  $|0\rangle$ .

scales like  $O(t^2)$ , which is a significant improvement over the proposal in [13].

We can consider this analysis a bit more carefully and determine upper bounds for the total number of single- and 2-qubit Clifford gates, and depth of the overall (PBC-compiled) quantum circuits within this framework. We construct the compiled circuits using only the Clifford generators:  $H$ ,  $S$  and CNOT. This is not a problem as the controlled- $Y$  and controlled- $Z$  operations used in our procedure can be easily written in terms of this set of gates using the identities:  $CY_{ij} = S_j^3 CX_{ij} S_j$  and  $CZ_{ij} = H_j CX_{ij} H_j$ . The maximum number of operations and depth arise in the case where each of the  $t$ -qubit Pauli operators has  $(t - 1)$  single-qubit  $Y$  operators and exactly 1 Pauli  $Z$  operator, for instance:  $P_1 = Z \otimes Y \otimes Y \otimes \dots \otimes Y$ ,  $P_2 = Y \otimes Z \otimes Y \otimes \dots \otimes Y$ , etc. These operators are all independent and pairwise commuting and give rise to an upper bound on the number of single-qubit Clifford generators which is  $N_{HS}^{ub} = 4t^2$  and an upper bound on the total number of CNOT gates given by  $N_{\text{CNOT}}^{ub} = t^2$ . As for the depth, the upper bound within this scheme is  $D^{ub} = t(t + 5) - 1$  layers. Evidently, these upper bounds will often be gross over-estimates of the actual depth and gate counts of the PBC-compiled circuits as the Pauli observables are commonly trivial in several of the qubits. This will be observed in the numerical results presented in section 4. Additionally, in that section, we will also confirm that this implementation of the PBC-compiled circuits frequently leads to reductions in the depth and gate counts needed to perform the computation. Moreover, we see that the number of qubits of the PBC-compiled circuits is reduced with respect to that of the original Clifford+ $T$  quantum circuit when-

ever  $t < n - 1$ .

A trade-off can be made between the depth of the PBC-compiled quantum circuits and the number of auxiliary qubits. In particular, we point out that it is possible to reduce the depth of the computation from  $O(t^2)$  to  $O(t \log t)$  at the expense of requiring  $t$  auxiliary qubits (instead of just 1). In this case, the number of qubits of the PBC-compiled circuits is only lower than that of the original circuit if  $2t < n$ . Nevertheless, even if this condition is not met, reducing the depth is a worthy goal in itself as it reduces the demands on the coherence time of the qubits. Therefore, which of the two approaches is better suited to practical implementation will vary on a case-by-case basis.

To decrease the depth of the compiled (adaptive) quantum computation from  $O(t^2)$  to  $O(t \log t)$ , we apply the following procedure in order to measure a  $t$ -qubit Pauli operator  $P_i = \sigma_{i;1} \otimes \sigma_{i;2} \otimes \dots \otimes \sigma_{i;t}$ :

1. Initialize the  $t$  auxiliary qubits in the GHZ state  $|GHZ_t\rangle = (|0\rangle^{\otimes t} + |1\rangle^{\otimes t})/\sqrt{2}$ . Such state can be generated by a quantum circuit  $\mathcal{U}$  of depth  $O(\log t)$  as depicted in Figure 2 of [32].
2. For each  $\sigma_{i;j}$  in  $P_i$  apply a controlled- $\sigma_{i;j}$  operation from the auxiliary qubit  $j$  to the main qubit  $j$ . Clearly, this can now be done in a single layer.
3. Next, apply  $\mathcal{U}^\dagger$  to the  $t$  auxiliary qubits (this requires  $O(\log t)$  additional layers).
4. Finally, measure the first auxiliary qubit to obtain the outcome  $s_i$  of  $P_i$  and leave the main qubits in the proper  $(-1)^{s_i}$ -eigenstate of that operator.

It is clear that the procedure described above allows for the measurement of any  $t$ -qubit Pauli observable via a circuit of depth  $O(\log t)$ . Since there are at most  $t$  such operators in the PBC sequence, the compiled circuit will have a depth which scales as  $O(t \log t)$ , as promised.

Note that the total number of operations in this approach still scales as  $O(t^2)$ , but the use of the  $t$ -qubit GHZ state allows the controlled- $\sigma_{i,j}$  operations in each Pauli to be carried out simultaneously (in a single layer) making the circuit shallower and significantly reducing the demands on the coherence time of the qubits.

As a final comment, we would like to point out once more that PBC compilation may significantly reduce the depth and gate count of a given input circuit. This is because the compiled circuits have a standard form, corresponding to at most  $t$  Pauli measurements. As we have seen, this standard form has strict and easy to derive bounds on gate count and depth, and which do not depend on the number of qubits, depth or Clifford gate count of the original circuit, but only on the number of  $T$  gates. This feature will be clear in the numerical results presented in the next section.

## 4 Practical contributions and numerical results

### 4.1 Efficiency and complexity

Besides the theoretical proposals presented in the previous section, we wrote Python code that actually performs the compilation of Clifford+ $T$  circuits with  $t$   $T$  gates, reducing the quantum computation to a standard PBC on  $t$  qubits, assisted by polynomial classical processing (as described in subsec. 2.3). This code can be found at <https://github.com/fcrperes/CompHybPBC>, together with some helpful documentation and toy examples. We defer any specific details of our code implementation to that repository. In here, it is only important to point out that the input quantum circuit must be unitary and written in terms of the Clifford generators  $H$ ,  $S$ , and CNOT, together with the  $T$  gate. Moreover, in alignment with the discussion above, the final quantum computation will be implemented using only these Clifford generators, and the first of our two proposed schemes.

Unfortunately, the possibility to run quantum circuits incorporating classical computation interleaved with quantum operations is not yet publicly available. This left us facing a technological limitation as we were unable to actually implement the compiled, adaptive computation in actual quantum hardware. However, a reader with access to such technology can easily adapt our code to actually carry out our proposed simulation scheme. At any rate, according to IBM’s roadmap [33], *dynamic* quantum circuits will become publicly available by the end of 2022, at which time our code can be easily used (at least) with these quantum chips by anyone who would like to explore this tool.

At present, however, and to circumvent the aforementioned limitation, we settled for a simple proof-of-principle, resorting to Qiskit’s Statevector Simulator [34], a Schrödinger-type simulator that we use to store and update the wavefunction after each circuit slice. This creates memory and runtime limitations for this proof-of-principle, but those constraints will be removed as soon as dynamic quantum/classical computation is made available, requiring only the rewriting of a single function in our code.

Having the future deployment of these techniques in real quantum hardware in mind, it is clear that the feasibility of PBC compilation demands that it be carried out within the coherence time of the qubits. Thus, in the next subsection we will assess the total runtime of our code, dividing it in what we call the classical and quantum runtimes. The former comprises the time it takes to carry out all the (polynomial) classical side-processing in a single shot of the PBC compilation procedure, while the latter refers to the time it takes to execute the actual quantum job (also per shot). Because, as explained above, our prototype is not integrated with a real QPU, we focus our analysis on the classical runtime of our code.

We have claimed multiple times that the classical processing carried out during the PBC compilation procedure takes polynomial time. We will now discuss this in a bit more detail, for the particular case of our implementation. As we have seen, the first step of the compilation procedure consists of assessing whether the current Pauli operator commutes or anti-commutes with any operator of the list of previously measured, inde-

pendent and pairwise commuting Pauli operators. In our implementation, this is done in  $O(t \cdot (n+t))$  time in the worst case and in  $O(n)$  time at best. As we have seen, if the Pauli observable indeed anti-commutes with any previously measured operator, we need only make a coin toss to ascertain its outcome, compute the Clifford operator  $V$ , and add it to the circuit. This is done in time  $O(n+g+t+m)$ , where  $m$  and  $g$  are, respectively, the number of measurements and Clifford gates in the original Clifford+ $T$  circuit; in doing this, the assessment of that Pauli observable is completed, allowing us to move on to the next one. However, if the Pauli commutes with all previously measured Pauli operators, we have seen that it is necessary to verify if it is dependent on or independent of those Pauli operators. Carrying out this task has a cost that scales like  $O(t^3+t \cdot (n+t))$  in the worst case. The cubic behaviour in  $t$  is the main complexity bottleneck of our code, and stems from performing Gaussian elimination in the  $GF(2)$  finite field following the algorithm described in [35].

Considering the entire PBC compilation procedure, the worst case cost of updating a single Pauli operator is  $O(t^3 + (n+t) \cdot (t+m) + n + t + g + m)$ . Since there is a total of  $(t+m)$  Pauli operators that need to be propagated through the circuit and assessed at the end, the total cost of the computation is, in the worst case,

$$O\left((t+m) \cdot (t^3 + (n+t) \cdot (t+m) + g)\right).$$

Assuming the situation where  $m = n$ , this simplifies further to:

$$O\left(t^4 + n \cdot t^3 + (n+t)^3 + g \cdot (n+t)\right). \quad (5)$$

This equation gives a behaviour for the classical runtime that is quartic in  $t$ , cubic in  $n$  and linear in  $g$ . However, it is important to point out that the costs presented are the worst-case costs, computed assuming the largest possible size of the matrix that stores in its rows the independent and pairwise commuting Pauli operators measured up until a given point in the PBC procedure. It is clear that the size of this matrix grows as the computation progresses (i.e. as we find new independent and pairwise commuting Pauli operators) so that earlier steps are much cheaper than estimated and, thus, the amortized cost of the

computation is lower than the results presented above. This is clear from the numerical results for the time of the classical processing presented below (cf. Figures 4 and 7).

The discussion presented above applies to the PBC compilation procedure together with the task of weak simulation. From sub-subsection 2.3.2, it is clear that things change slightly for the task of hybrid PBC. Evidently, the compilation procedure is still an integral part of that task, retaining its polynomial efficiency and cost (but with  $m = 1$ ). However, we now need to compile  $3^k$  different input quantum circuits, each of which needs to be sampled a given number of shots  $N$  determined by the maximum desired error  $\epsilon$ . Therefore, it is clear that we now have an exponential demand on the side of the quantum hardware and also, inevitably, on the overall classical processing. Given this exponential overhead, it is fair to ask ourselves whether this approach brings any advantage over the full classical simulators discussed in subsection 2.1. Considering those based on stabilizer-rank techniques, we have seen that the best known scaling of such simulators for the task of strong simulation is  $O(2^{0.3693t})$ . Considering this asymptotic behaviour and comparing it against the one achieved with hybrid PBC, we see that our approach is asymptotically advantageous whenever  $k \lesssim t/4$ .<sup>5</sup>

To benchmark our code we run it on a remote server with a total available memory of 32 GB and 8 Intel(R) Xeon(R) CPU E3-1270 v5 @ 3:60 GHz processors each with 4 CPU cores. We start by considering the problem of sampling from the output distribution of the given input quantum circuits, and afterward we consider the task of carrying out approximate strong simulation with different relative errors and different numbers of virtual qubits. For these two distinct tasks we benchmark our simulations by considering first hidden-shift circuits (HSCs), followed by random quantum circuits (RQCs).

We would like to conclude by pointing out that the main goal of our code is to materialize the abstract and conceptual ideas of PBC into a practical solution for compiling Clifford+ $T$  quantum circuits. Therefore, the runtime of our code can

<sup>5</sup>Evidently, this comparison is a bit over-simplistic in the sense that it disregards important considerations of practical nature, such as, for instance, the presence of noise in a real quantum device.

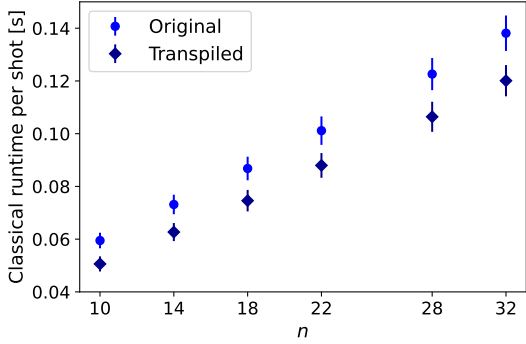


Figure 4: Classical runtime for hidden-shift circuits with  $n$  qubits and 14  $T$  gates. Time required for the classical processing that accompanies a single-shot (standard) Pauli-based computation for both the original (light blue circles) and the pre-compiled (dark blue diamonds) hidden-shift circuits featuring 14  $T$  gates, as a function of the number of qubits  $n$ . The total computational runtime for each PBC shot will be this classical runtime added to the time taken by the QPU.

certainly be significantly improvable via more sophisticated software-engineering techniques, not to mention the use of a different programming language like C++ or Julia.

## 4.2 Task 1: Compilation and weak simulation

To analyse the performance of our compilation code, each input Clifford+ $T$  unitary quantum circuit is compiled and simulated for a total of 1024 shots, and we evaluate the classical processing time per shot, as well as the total single- and 2-qubit gate counts, and depth obtained for each compiled circuit.

### 4.2.1 Hidden-shift circuits

Hidden-shift circuits (HSCs) have been frequently used in the literature to benchmark the performance of full classical simulators using stabilizer-rank-based techniques [22, 23, 26]. This is because, on the one hand, they are naturally written in terms of the Clifford+ $T$  gate set and, on the other hand, they are deterministic, so that the outcome of the simulator can be verified against the correct outcome (known *a priori*).

The family of HSCs considered in this paper is that of Clifford+ $T$  circuits with an even number of qubits,  $n$ , a hidden string,  $\mathbf{s}$ , which is returned deterministically, and the following structure:

$$C = H^{\otimes n} O_{f'} H^{\otimes n} O_f H^{\otimes n}, \quad (6)$$

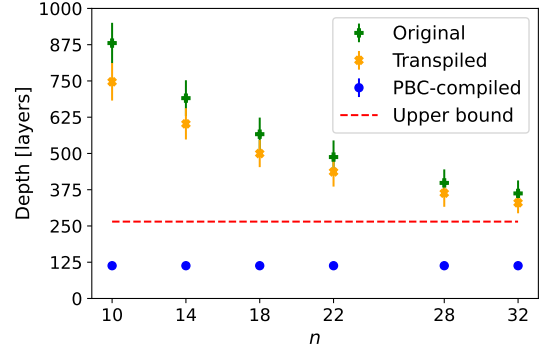


Figure 5: Depth of the original (green), and pre-compiled (orange) hidden-shift circuits with 14  $T$  gates, and of the PBC-compiled circuits (blue), as a function of the number of qubits  $n$  of the original circuits. The dashed red line represents the upper bound for the depth of the (standard) PBC ( $D^{ub} = t(t+5) - 1 = 265$ ) and, as expected, it is much larger than the actual depths of the compiled circuits.

where  $O_f$  and  $O_{f'}$  are the two  $n$ -qubit oracles of the hidden-shift algorithm given by:

$$O_f = \left( \prod_{i=1}^{n/2} CZ_{i,i+n/2} \right) (O_g \otimes I) \quad (7)$$

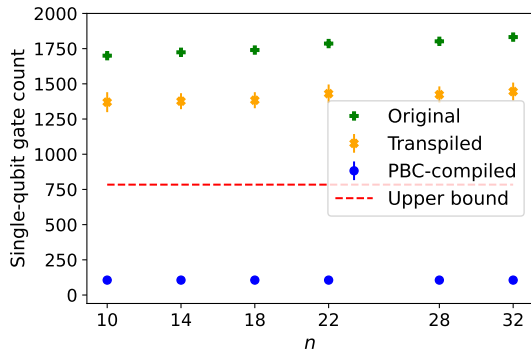
and

$$O_{f'} = \left( \prod_{i=1}^{n/2} CZ_{i,i+n/2} \right) (I \otimes O_g) Z(\mathbf{s}). \quad (8)$$

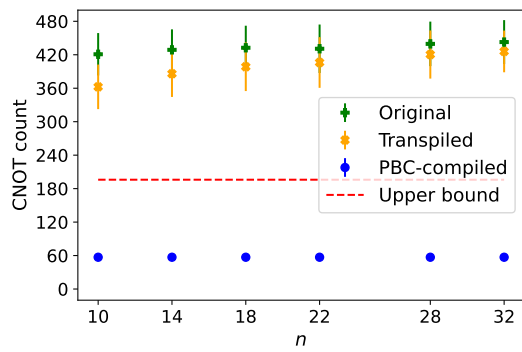
Here,  $Z(\mathbf{s}) = Z^{s_1} \otimes Z^{s_2} \otimes \dots \otimes Z^{s_n}$  and  $O_g$  is an  $n/2$ -qubit unitary defined by the number of  $CCZ$  gates,  $N_{CCZ}$ , used to construct it and by the number of  $\{Z, CZ\}$  gates,  $N_{Z,CZ}$ , within each  $\{Z, CZ\}$ -segment placed at the beginning and at the end of  $O_g$ , and in-between every  $CCZ$  gate.<sup>6</sup> This structure implies that there are  $N_{CCZ} + 1$   $\{Z, CZ\}$ -segments, each of which is built by drawing  $N_{Z,CZ}$  gates uniformly at random from the  $\{Z, CZ\}$  gate set, and acting with each drawn gate on a randomly chosen qubit or qubits. The three qubits involved in each  $CCZ$  are also drawn randomly from the set of  $n/2$  qubits acted on by  $O_g$ .

This family of HSCs is that defined in [22], with two major differences. First, after generating the circuits, the  $Z$  and  $CZ$  gates need to re-written in terms of the (allowed) Clifford generators:  $Z_i = S_i^2$  and  $CZ_{ij} = H_j CX_{ij} H_j$ . Secondly, the  $CCZ$  gate can be written in terms of

<sup>6</sup>Note that equations (7) and (8), and the oracle  $O_g$  demand that  $n$  be an even number.



(a) Number of single-qubit gates of the original (green), and pre-compiled (orange) hidden-shift circuits with 14  $T$  gates, and of the PBC-compiled quantum circuits (blue), as a function of the number of qubits  $n$  of the original circuits. The dashed red line represents the upper bound for this quantity ( $N_{HS}^{ub} = 4t^2 = 784$ ) and, as expected, it is much larger than the actual final values.



(b) CNOT count of the original (green), and pre-compiled (orange) hidden-shift circuits with 14  $T$  gates, and of the PBC-compiled quantum circuits (blue), as a function of the number of qubits  $n$  of the original circuits. The dashed red line represents the upper bound for this quantity ( $N_{CNOT}^{ub} = t^2 = 196$ ) and, as expected, it is much larger than the actual final values.

Figure 6: Gate counts for the original (green), and pre-compiled (orange) hidden-shift circuits with 14  $T$  gates, and for the PBC-compiled quantum circuits (blue), as a function of the number of qubits  $n$  of the original (input) circuits.

the Toffoli gate, for which we then considered the optimal, non-adaptive decomposition as proposed by Shende and Markov in [36]. As a consequence, our circuits have a  $T$ -count which is  $t = 14N_{CCZ}$ . For this reason, and due to limitations associated with the Schrödinger-type simulator, we examined only circuit instances with  $t = 14$ . For more details about this family of circuits, the reader is encouraged to read the supplementary material of [22].

We used input Clifford+ $T$  circuits with different total numbers of qubits:  $n = \{10, 14, 18, 22, 28, 32\}$ , and for each  $n$  generated a single hidden string  $\mathbf{s}$  at random from the  $2^n$  possible strings. As explained above, the structure of the generated circuits guarantees that their output is deterministic and corresponds to the generated string:  $y_{out} = \mathbf{s}$ . Evidently, the same result is output by our code.

For each of the six values of  $n$ , we generated and simulated 100 different HSCs. For completeness, we further decided to analyse what would happen if we pre-compiled the input quantum circuits with another tool before using our code. To that end, we used Qiskit’s transpiler, although there is nothing special about this particular pre-compilation, and other tools could be used instead before running our code.

We expect that by pre-compiling the quantum circuits, the time of the classical processing is lowered as the number of gates through which the

Pauli operators need to be propagated is reduced *a priori*. This is corroborated by the results presented in Figure 4.

Note that the PBC-compiled (adaptive) quantum circuits require  $t + 1 = 15$  qubits, that is, our compilation code yields a reduction of the number of qubits only for the input circuits with  $n > 16$ . In contrast, all other resources, i.e. depth and gate counts, are reduced with respect to those of the original circuits (cf. below).

In Figure 5, we see a substantial depth reduction provided by the use of our (adaptive) PBC scheme. Specifically, the compiled quantum circuits have one of five possible depths: 111, 112, 113, 114, or 115. These values are around 2.3 times smaller than the respective upper bound, and between 2.8 and 8.6 times smaller than the depths of the original (input) quantum circuits.

As for the gate counts, the reductions are also striking (see Figure 6). The total number of single-qubit gates reaches values between 6.5 and 8.5 times smaller than the corresponding upper bound and between 14 and 20 times smaller than those of the original quantum circuits. On the other hand, the total number of controlled-NOT gates in the compiled quantum computations is always either 56, 57 or 58; these values are roughly 3.4 times smaller than the corresponding upper bound, and between 6.6 and 8.6 times lower than those of the original quantum circuits.

All in all, our code achieves some promising

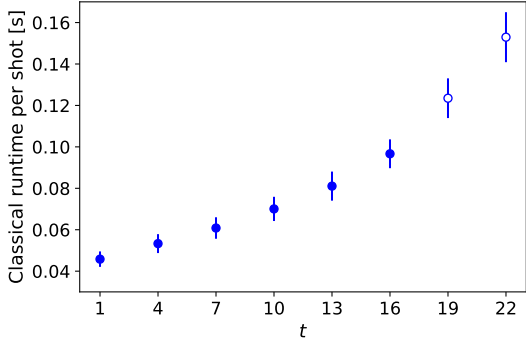


Figure 7: Classical runtime for random quantum circuits with 25 qubits and  $t$   $T$  gates. Time required for the classical processing that accompanies a single-shot (standard) Pauli-based computation for random quantum circuits with 25 qubits, as a function of the  $T$ -count  $t$  of the original circuits. The total computational runtime for each PBC shot will be this classical runtime, added to the time taken by the QPU. The last two points are depicted as white-faced circles to highlight the fact that for these two values of  $t$  we have simulated only 5 circuits (instead of 100).

reductions of the quantum resources necessary to implement the desired computation, while requiring a classical processing which is only of the order of hundreds of milliseconds per shot. These results are encouraging especially in light of the fact that this classical runtime should be significantly improvable. Moreover, it is worth pointing out that even if the input quantum circuits are generated using a larger number of  $Z$  and  $CZ$  gates, thus having larger depth and gate counts, we still expect the final (adaptive) compiled computation carried out by our code to reach the same numerical results as the ones presented in Figures 5 and 6. As explained at the end of section 3, the reason for this is the underlying, strict standard form of the compiled computation, which depends only on the structure of the original circuit and on its  $T$ -count.

#### 4.2.2 Random quantum circuits

Having verified that our code works flawlessly with the HSCs, outputting the correct deterministic result, we now turn our attention to the case of random input Clifford+ $T$  quantum circuits. To complement the data obtained with the HSCs, we generated random circuits with a fixed number of qubits  $n = 25$ , but varying  $t = \{1, 4, 7, 10, 13, 16, 19, 22\}$ . This generation was strongly inspired by the random quantum cir-

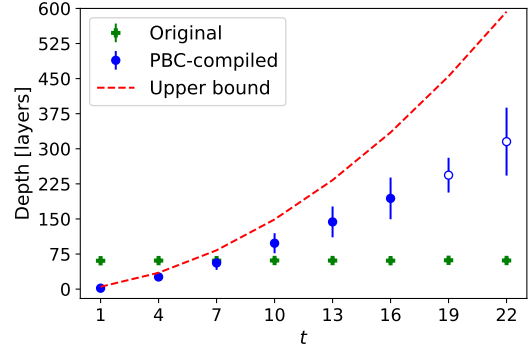
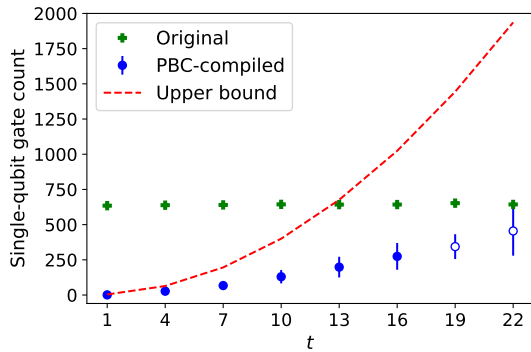


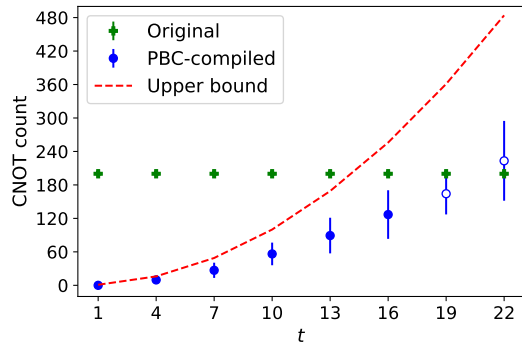
Figure 8: Depth of the input random quantum circuits with 25 qubits (green) and of the compiled quantum circuits (blue), as a function of the  $T$ -count,  $t$ , of the original circuits. The dashed red line represents the upper bound for the depth of the PBC ( $D^{ub} = t(t+5) - 1$ ). The last two points are depicted as white-faced circles to highlight the fact that for these two values of  $t$  we have simulated only 5 circuits (instead of 100).

cuits (RQCs) proposed in [37]:

1. The  $n = 25$  qubits are initialized in the state  $|0\rangle^{\otimes n}$ .
2. The first layer of the circuit consists of Hadamard gates acting on all qubits:  $H^{\otimes n}$ .
3. The next  $N_{cycles}$  layers are generated by picking up 1 out of the 8 possible entangling configurations presented in Figure 2a of [37]. This is motivated by practical constraints in qubit connectivity, assuming a device that has a rectangular-grid configuration so that the  $n$  qubits are arranged in an  $(n_c \times n_r)$ -grid. This means that  $n = n_c \cdot n_r$ , where  $n_c$  and  $n_r$  denote, respectively, the number of columns and rows in the grid. Our circuits assume a  $(5 \times 5)$ -grid structure and were generated with  $N_{cycles} = 40$ . Note that the entangling gate used is the controlled- $Z$  gate.
4. For each layer, each qubit that is not acted on by a  $CZ$  gate will be acted on by a single-qubit gate drawn from the  $\{S, H, T\}$  gate set. The drawing of such gates should follow the ensuing rules:
  - (a) the probability  $p(T)$  of drawing  $T$  is adjusted so that, in the end, the total number of  $T$  gates is (close or equal to) the desired one;
  - (b) the probability of drawing either one of the other two gates is the same and



(a) Number of single-qubit gates of the input 25-qubit random quantum circuits (green) and of the (respective) compiled quantum circuits (blue), as a function of the number of  $T$  gates,  $t$ , of the original circuits. The dashed red line represents the upper bound for this quantity ( $N_{HS}^{ub} = 4t^2$ ). The last two points are depicted as white-faced circles to highlight the fact that for these two values of  $t$  we have simulated only 5 circuits (instead of 100).



(b) CNOT count of the input 25-qubit random quantum circuits (green) and of the (respective) compiled quantum circuits (blue), as a function of the number of  $T$  gates,  $t$ , of the original circuits. The dashed red line represents the upper bound for this quantity ( $N_{CNOT}^{ub} = t^2$ ). The last two points are depicted as white-faced circles to highlight the fact that for these two values of  $t$  we have simulated only 5 circuits (instead of 100).

Figure 9: Gate counts of the original 25-qubit random quantum circuits (green) and of the PBC-compiled quantum circuits (blue), as a function of the  $T$ -count,  $t$ , of the original circuits.

given by  $p(S) = p(H) = (1 - p(T))/2$ .

A post-selection criterion is placed on the generated samples to ensure that they have the desired number of  $T$  gates.

5. In the end, all qubits are measured in the computational basis so that  $m = n = 25$ .

Note that unlike the set-up in [37], here we do not demand that the first single-qubit gate acting on each qubit (after the initial  $H^{\otimes n}$  layer) be a  $T$  gate. This is important because it allows more flexibility in the number of  $T$  gates in the circuit. Additionally, and also unlike [37], our set-up might allow the commutation of some gates and the simplification of the quantum circuits. For this reason, two more steps were taken before feeding these circuits as input to our code:

1. The entangling  $CZ$  gates were transformed into CNOTs.
2. We made a pre-compilation of these circuits, using gate commutativity and circuit identities to remove disposable gate sequences. After this, the total  $T$ -count of the circuit must remain the desired one, or else that circuit is discarded.

Here, the values of  $n$  and  $t$  imply that all RQCs are compiled to instances with lower qubit counts. Just like for the HSCs, we simulated 100 different

RQCs for  $t$  from 1 up to 16. However, for the last two  $T$ -count values, time constraints (related to the Statevector simulator) led us to simulate only 5 different random circuits. For this reason, the corresponding data points in the figures are distinguished from the others by being represented by empty circles (instead of filled ones).

Figure 7 depicts the classical time associated with the compilation procedure as a function of the number of non-Clifford gates in the original circuits. Just as before, this time is around hundreds of milliseconds per shot, but we expect this to be significantly improvable. Also noteworthy here is the fact that the behaviour of the classical processing time as a function of  $t$  is considerably different from that seen with  $n$  (cf. Figure 4). Specifically, the classical runtime scales much faster with  $t$  than with  $n$ , as was to be expected from the discussion in subsection 4.1.

We can see the depth associated with these compiled circuits in Figure 8. In this case, and contrary to what happened with the HSCs, we see that for  $T$ -counts larger than  $t = 7$  the depth of the PBC-compiled computations is actually larger than that of the original circuits. However, it is important to notice that if we use a larger number of layers,  $N_{cycles}$ , we will increase the depth of the original computation without having any effect on the depth of the final (PBC-compiled) circuits.

We also see, from Figure 9, that despite their larger depth for  $t > 7$ , the total gate counts of the PBC-compiled circuits are still smaller than those of the original Clifford+ $T$  quantum circuits. (The exception to this is the CNOT count for  $t = 22$ .) This shows that in terms of the quantum gates required for the actual quantum computation, our approach is still favorable, although it might be deeper due to the particular form of the implementation scheme we are using. In fact, these results suggest that these RQCs are instances which might benefit from the qubit-count/depth trade-off provided by our second proposed scheme.

Finally, we should once more reinforce the idea that if the original quantum circuits are made to be larger (for instance due to an increase of the grid size and/or of the number of cycles), the size of the compiled circuits will remain essentially unchanged as long as the value of  $t$  is maintained.

#### 4.2.3 Dummy simulation and larger circuits

In order to verify what happens for larger quantum circuits, we included in our code the possibility to run a *dummy* simulation of the actual quantum measurements of the standard PBC. This dummy simulation works by simply making a coin toss to ascertain the outcome of each Pauli observable that should be measured in the QPU. It is clear that, in doing so, we are not making a correct weak simulation of the original circuit, i.e. we are not sampling from the correct output distribution. This is because we will explore paths down the PBC tree that would not occur in the real simulation, or that would occur with different probability.

Nevertheless, using this dummy simulator allows us to use our code to compile quantum circuits with larger  $T$ -counts than those allowed by the use of the real Schrödinger-type simulator and, thus, get a prediction for the features of the PBC-compiled circuits (depth and gate counts), as well as for the time of the classical processing for those instances. Despite the fact that the PBC tree will not be explored correctly, yielding a wrong weak simulation of the original circuit, we have verified that this dummy simulator reliably estimates the final features of the compiled quantum circuits. We did this by simulating the same hidden-shift and random quantum circuits as compiled with the real simulator in the previous two sub-subsections.

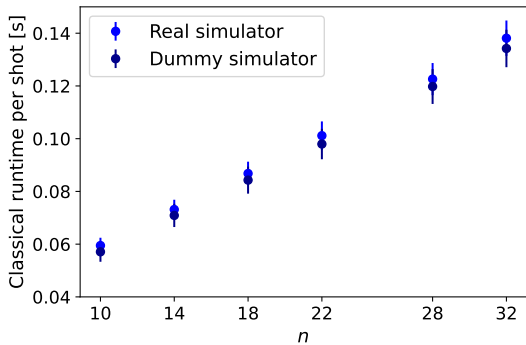
In the case of the HSCs, we clearly see the effect of sampling from the incorrect probability distribution, as the output is no longer deterministic. Nevertheless, the results for the depth and gate counts were (essentially) the same as obtained with the real Schrödinger-type simulation. The same holds for the results associated with the RQCs.

On the other hand, it was interesting (and somewhat surprising) to observe that the estimates of the classical runtime are different when we use the real, Schrödinger-type simulator and the dummy simulator. This can be seen in Figure 10. For the HSCs, the differences are small (between 2 and 4ms) and negligible, since they are lower than the width of the confidence intervals; they also seem to be approximately constant (or else varying quite slowly) with  $n$  (cf. Figure 10a). In contrast, for the RQCs, as the  $T$ -count increases, the discrepancy between the classical runtime per shot estimated using the Schrödinger-type or the dummy simulator also increases (cf. Figure 10b).

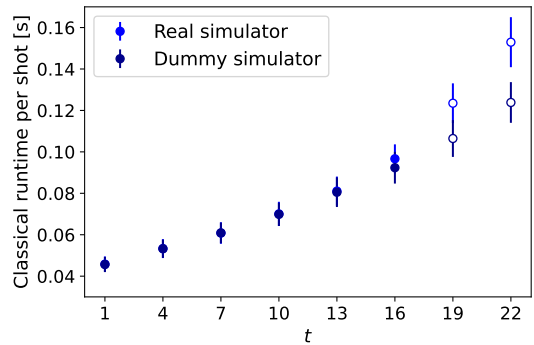
From our point of view, there might be two factors at play, contributing to these observed differences. First, they may be precisely due to the fact that different PBC paths are run through with incorrect probability when using the dummy simulator, requiring different computational efforts. However, we believe that such should be a very small contribution, of only a couple of milliseconds, as observed for instance for the HSCs. The second, and probably larger factor, comes from the overwork incurred on the classical machine due to the highly demanding Schrödinger-type circuit simulation. One strong argument to support this claim is the fact that, contrary to what happens with  $n$ , the discrepancies increase visibly with  $t$ , which is the variable that determines the hardness of the simulation for the real, Schrödinger-type simulator. For this reason, we expect that the time of the classical processing is better, even if not perfectly, estimated by the use of the dummy simulator.

Since the dummy simulator can be used to reliably estimate the properties of these PBC-compiled quantum circuits, we decided to employ it in our code to study the results of the compilation procedure when applied to input quantum circuit instances with larger numbers of  $T$  gates.

We started by using this set-up to compile a



(a) Classical runtime for hidden-shift circuits with  $n$  qubits and 14  $T$  gates. Time required for the classical processing that accompanies a single-shot (standard) Pauli-based computation for the original hidden-shift circuits featuring 14  $T$  gates, as a function of the number of qubits  $n$ , when using the (real) Schrödinger-type simulator (light blue) and the dummy simulator (dark blue).



(b) Classical runtime for random quantum circuits with 25 qubits and  $t$   $T$  gates. Time required for the classical processing that accompanies a single-shot (standard) Pauli-based computation for random quantum circuits with 25 qubits, as a function of the  $T$ -count,  $t$ , of the original circuits, when using the (real) Schrödinger-type simulator (light blue) and the dummy simulator (dark blue). The last two data-points are depicted as white-faced circles to highlight the fact that for these two values of  $t$  we have simulated only 5 circuits (instead of 100).

Figure 10: Time of the classical processing for (a) a set of hidden-shift circuits and (b) a set of random quantum circuits, when using the (real) Schrödinger-type simulator (light blue) and the dummy simulator (dark blue).

set of 50 HSCs with 42 qubits and 42  $T$  gates, generated as explained in sub-subsection 4.2.1. The classical processing time per shot required to compile one of these circuits can be found within the 95% confidence interval  $\tau_{cl.} = (0.58 \pm 0.02)$ s. Clearly, this value is too demanding for current NISQ devices; however, as has been mentioned several times, this classical processing time should be significantly improvable.

Regarding the properties of the original and compiled quantum circuits, we start from instances with depth  $d_{orig.} = (568 \pm 64)$  and these are compiled to circuits with depth  $d_{comp.} = (357 \pm 25)$ ; this corresponds to reductions in the depth between 24% and 48%. For the gate counts, we start from circuits with 3572 single-qubit gates, and end up with compiled circuits with  $N_{HS;comp.} = 350 \pm 47$ , which corresponds to a reduction between 89% and 92%. Finally, the CNOT gate count changes from  $N_{CNOT;orig.} = 881 \pm 54$  to  $N_{CNOT;orig.} = 187 \pm 26$ , amounting to a reduction between 74% and 83%.

These results show that our PBC compilation is very successful in reducing the quantum resources required to carry out the computation encoded by the hidden-shift circuits of the considered family, both for smaller and larger instances.

Next, we decided to consider again the case of random quantum circuits with  $n = 25$ . As ex-

plained before, input circuits with a larger number of qubits will have the same depth (as long as  $N_{cycles}$  is unchanged) and larger gate counts; on the other hand, the compiled circuits will have essentially the same properties, as the PBC structure is insensitive to changes in the total number of qubits in the grid. For  $n = 25$  and  $N_{cycles} = 40$ , we have seen that the compiled circuits start being deeper than the original ones for  $t \gtrsim 7$ . Using the dummy simulator, we compiled circuit instances with larger  $t$  and  $N_{cycles}$  to set up an approximate boundary line which determines for each  $N_{cycles}$  the value of  $t$  below which the PBC compilation leads to circuits that are shallower than the original one.

We can easily derive a lower bound for this boundary line. To that end, recall that the upper bound on the depth of the PBC-compiled circuits is such that  $d_{PBC} \leq t^2 + 5t - 1$  (cf. section 3). Next, we note that, when written in terms of the Clifford generators, the depth of the original Clifford+ $T$  RQCs necessarily obeys the condition  $d_{orig.} \geq N_{cycles} + 2$ . Combining these two conditions, we get a lower bound for the boundary line such that:

$$t \geq -\frac{5}{2} + \frac{1}{2}\sqrt{4N_{cycles} + 37}. \quad (9)$$

Thus, we have  $t \sim \Omega(\sqrt{N_{cycles}})$ . More than that,

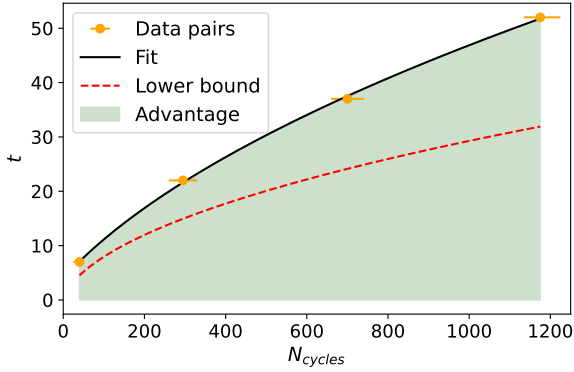


Figure 11: Region of advantage of PBC compilation for random quantum circuits on 25-qubits, with respect to depth. The orange data points represent the  $(N_{cycles}, t)$ -pairs for which the respective random quantum circuits and their PBC compilation have the same depth. These points result from compiling circuits with  $(N_{cycles}, t) = \{(22, 7), (295, 22), (700, 37), (1175, 52)\}$  using the dummy simulation option in our code. The black line is obtained by fitting a square-root function to the four data points. This boundary line is consistent with the lower bound (dashed red curve) determined in the main text. The green region corresponds to random-circuit parameters for which PBC compilation decreases the depth, whereas circuits in the white region have their depth increased by PBC compilation.

we still expect the boundary line to be such that  $t \sim \sqrt{N_{cycles}}$ , albeit with coefficients that bring it (necessarily) above the lower bound.

These predictions seem to be corroborated by Figure 11. To obtain this figure, we compiled four sets of 100 quantum circuits with  $(N_{cycles}, t) = \{(22, 7), (295, 22), (700, 37), (1175, 52)\}$ . For each of these pairs, the average depth of the PBC-compiled circuits matches that of the original circuits. This gave us the orange data points depicted in Figure 11. From the previous subsection, we understand that the depth of the PBC-compiled circuit is better defined by a confidence interval than a single value. The lower and upper bounds of that interval allow us to find lower and upper bounds for the value of  $N_{cycles}$  of the original circuits which are still compatible with the confidence interval of the depth of PBC-compiled circuits. This gave us the uncertainty bars depicted in orange in Figure 11.

The black line depicted in this same figure was constructed by fitting a square-root curve to the four data points. This line corresponds to the set of  $(N_{cycles}, t)$ -pairs for which PBC compilation

does not change the depth with respect to that of the original circuits. As expected, the quality of the fit is good, meeting our expectation that  $t \sim \sqrt{N_{cycles}}$ ; additionally, the curve respects the derived lower bound (dashed red line).

The green region highlights the set of  $(N_{cycles}, t)$ -pairs that define random circuit instances whose PBC-compiled quantum circuits will be shallower than the original. Note that these results should be independent of the number of qubits in the original RQCs.

To conclude, we would like to note that the classical runtime per shot for the larger RQCs was  $\tau_{cl.} = (2.5 \pm 0.2)s$ . By construction, the depth of the original circuits corresponds to the depth of the PBC-compiled instances. As for the gate counts, the original circuits had respectively  $18\,309 \pm 219$  and  $5\,875$  single- and 2-qubit gates, while the corresponding results for the PBC-compiled circuits were  $2\,092 \pm 129$  and  $1\,475 \pm 62$ .

### 4.3 Task 2: Virtual qubits and approximate strong simulation

In this section we will present the results obtained for the hybrid PBC set-up, where we simulate different numbers of virtual qubits and determine the probability  $p$  that a given qubit yields the outcome 1 with different precisions.

We start by considering one of the HSCs with  $n = 10$  belonging to the set of circuits used in Task 1. For this value of  $n$ , the hidden string is  $\mathbf{s} = 1001110010$ , so that each qubit has a deterministic output, that is, either  $p = 0$  or  $p = 1$ . We expect that hybrid computation allows to estimate this probability within relative error  $\epsilon$ . For this particular case, we run the hybrid PBC with different numbers of virtual qubits, namely 1, 2, 3, and 4, and with a fixed, maximum relative error of  $\epsilon = 0.1$ . Additionally, we consider a 95% confidence interval so that the coefficient  $c$  in equation (4) is  $c = \sqrt{20} \approx 4.47$ . In doing this we see that each of the  $M = 3^k$  different PBCs stemming from the decomposition in equation (2) needs to be run for a total of  $N = 1\,586, 1\,258, 997,$  and  $791$  shots, respectively for 1, 2, 3, and 4 virtual qubits. Thus, the total number of shots required to estimate the probability  $p$  of a given (specific) qubit for each of these numbers of virtual qubits is  $\mathcal{N} = 4\,758, 11\,322, 26,919,$  and  $64\,071$ . These and other numerical values are summarized in Ta-

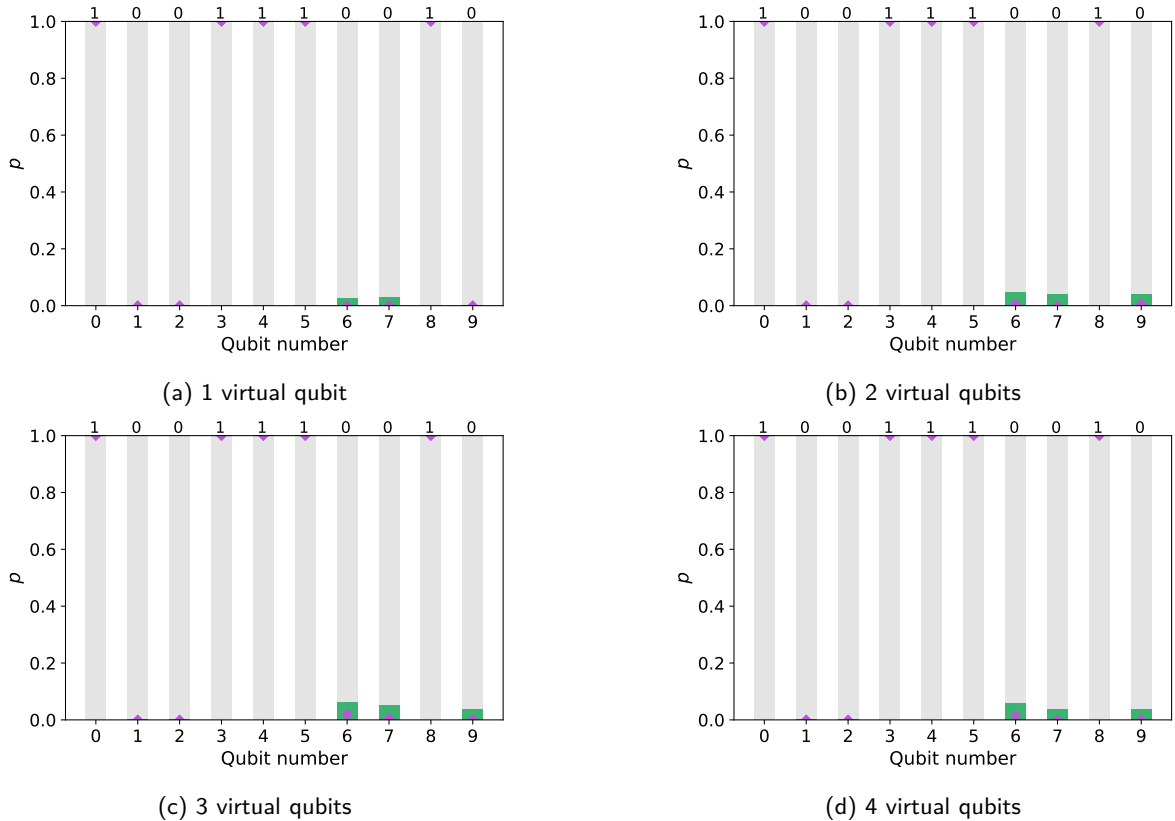


Figure 12: Probability of getting the outcome 1 for each of the 10 qubits of a (randomly chosen) hidden-shift circuit with 14  $T$  gates, for 4 different numbers of virtual qubits. The precision was set at  $\epsilon = 0.1$  so that the total number of shots (per qubit) is  $\mathcal{N} = 4758, 11322, 26919,$  and  $64071,$  respectively for 1, 2, 3 and 4 virtual qubits (cf. Table 1). The magenta diamonds represent the expectation value of the random variable  $\xi$  and the green bars correspond to 95% confidence intervals following Chebyshev’s inequality and using the standard deviation  $\sigma(\xi)$  of the actual data. For the qubits without such confidence intervals (i.e. qubits 0-5 and 8), the random variable  $\xi$  assumes the same value in all shots. That is, for these qubits  $\sigma(\xi) = 0$  and  $\mathbb{E}(\xi) \equiv p$ . At the top of each bar we see the correct deterministic output for each qubit. We note that all estimates of  $p$  are consistent with the correct output.

ble 1. The results are depicted in Figure 12. They illustrate how we can combine a classical machine and a small QPU to simulate a larger computation than allowed by the available quantum hardware. Specifically, we are simulating a PBC on 15 qubits via smaller PBCs involving, respectively, 14, 13, 12 and 11 qubits.

The structure of the different PBCs ensures that, for this particular circuit, the measurements of qubits 0-5 and 8 are each always mapped to the same trivial Pauli operators with the form:

$$P_i = \pm Z(\mathbf{a}) \bigotimes_{j=1}^t I, \quad (10)$$

where  $\mathbf{a} \in \{0, 1\}^n$ , and  $Z(\mathbf{a}) = Z^{a_1} \otimes \dots \otimes Z^{a_n}$ . Clearly, the outcome of such Pauli observables can be determined classically (step 3(b) of the PBC procedure described in subsection 2.3). Because each measurement of each of these qubits

is always mapped to the same observable, its outcome is always either 0 or 1, respectively for the positive or negative signs. Hence, the random variable  $\xi$  yields the same value (either 0 or 1) across all shots so that  $\sigma(\xi) = 0$  and  $\mathbb{E}(\xi) \equiv p$ . This means that the results for these qubits are independent of the chosen value of  $\epsilon$  or, equivalently, they are independent of the total number of shots. Consequently, we could use a smaller number of samples to estimate the value of the probability  $p$  associated with these qubits; in this extreme situation, wherein such information about the PBC structure can be known *a priori*, a single sample is sufficient to get the correct estimate of  $p$ .

Evidently, for the remaining qubits, if we decrease  $\epsilon$  we will see the corresponding confidence intervals narrowing further around 0. We omit such an illustration for this particular circuit, as

		$\epsilon = 0.1$		$\epsilon = 0.01$	
$k$	$M$	$N$	$\mathcal{N}$	$N$	$\mathcal{N}$
1	3	1 586	4 758	158 579	475 737
2	9	1 258	11 322	125 736	1 131 624
3	27	997	26 919	99 696	2 691 792
4	81	791	64 071	79 048	6 402 888

Table 1: Required number of samples as a function of the number of virtual qubits,  $k$ , and of the desired maximum relative error,  $\epsilon$ . Here,  $M = 3^k$  is the total number of differently weighted PBCs arising from the stabilizer pseudomixture in equation (2),  $N$  is the required number of shots for each of these PBCs, and  $\mathcal{N} = M \cdot N$  is the total number of shots for a given pair  $(k, \epsilon)$ . The values of  $N$  were computed considering a 95% confidence level so that, in equation (4),  $c = \sqrt{20} \approx 4.47$ . Note that these numbers are valid for both hidden-shift and random quantum circuits, as well as any other input circuit.

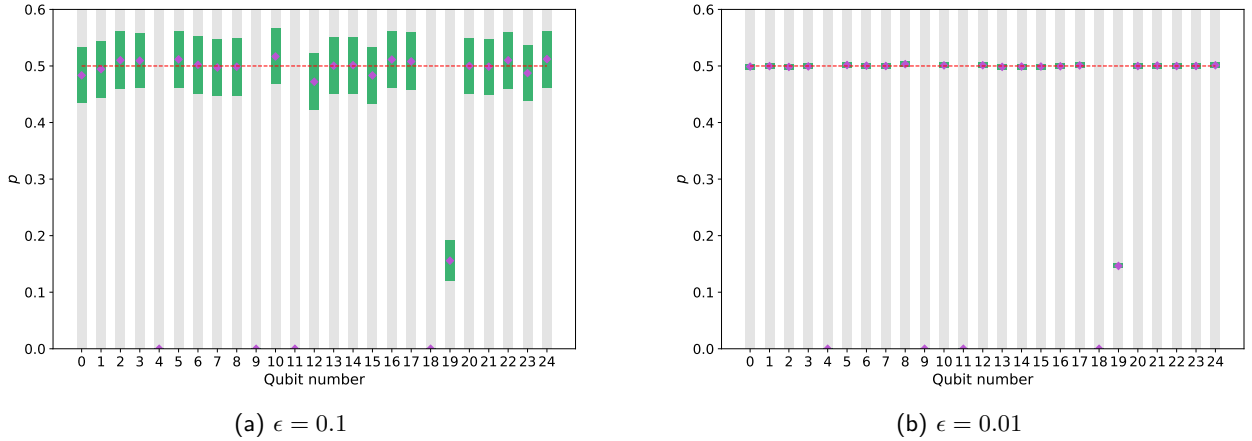


Figure 13: Probability of getting the outcome 1 for each of the 25 qubits of a (randomly generated) random quantum circuit with 13  $T$  gates, for 2 different maximum error values: (a)  $\epsilon = 0.1$ , and (b)  $\epsilon = 0.01$ , and simulating a single virtual qubit. The total number of shots (per qubit) was 4758 and 475 737, respectively for  $\epsilon = 0.1$  and  $\epsilon = 0.01$  (cf. Table 1). The magenta diamonds represent the expectation value of the random variable  $\xi$  and the green bars correspond to 95% confidence intervals following Chebyshev's inequality and computed using the real standard deviation of the data,  $\sigma(\xi)$ . For qubits without such confidence intervals, the random variable  $\xi$  assumes the same value in all PBC shots so that  $\sigma(\xi) = 0$  and  $\mathbb{E}(\xi) \equiv p$ .

it will be done in the next case study.

As for Task 1, we would also like to illustrate this hybrid PBC set-up for the case of input RQCs. The circuits considered in sub-subsection 4.2.2 had  $N_{cycles} = 40$ . For this reason, these circuits are very well mixed and their output probability distribution is (almost perfectly) uniform for nearly all instances. This means that  $p \approx 0.5$  for (nearly) every qubit of each circuit.

To be able to run our hybrid PBC task and see deviations from this uniform behaviour we chose to generate a single random quantum circuit with  $n = 25$ , and  $t = 13$ , but with only  $N_{cycles} = 8$ . For that circuit, we estimated the output probability of each qubit using a Schrödinger-type simulator and obtained the following results:

- $p = 0$  for qubits 4, 9, 11, and 18;

- $p \approx 0.146$  for qubit 19;
- $p \approx 0.5$  for all other qubits.

We expect to obtain the same results by carrying out hybrid PBC. We did so for two different maximum errors:  $\epsilon = 0.1$  and  $\epsilon = 0.01$  and only a single virtual qubit. Under these conditions, and considering again a 95% confidence level, the total number of samples required to obtain the results was, respectively,  $\mathcal{N} = 4758$  and  $\mathcal{N} = 475 737$  (cf. Table 1). The results can be found in Figure 13.

As expected, the estimate of  $p$  obtained using hybrid PBC is consistent with the values presented above. The outcome 0 is deterministically output by our code for qubits 4, 9, 11, and 18. This is because these qubits are mapped to Pauli

observables of the form given by equation (10). As for the other qubits, the correct value of  $p$  is always included in the estimated confidence interval. In this case, we also see how reducing the maximum (allowed) error by a factor of 10 strongly narrows the intervals around the expectation value of  $\xi$ . These results were obtained when simulating a single virtual qubit, but similar results would be obtained for larger virtual-qubit counts.

## 5 Concluding remarks

We have shown how the Pauli-based model of quantum computation can be used in practice to compile a given unitary Clifford+ $T$  circuit. Compared to prior work [13], our first scheme reduces the number of quantum gates required to perform the computation, specifically, to  $O(t^2)$  instead of  $O(t^3/\log(t))$ , at the expense of requiring a single auxiliary qubit. Our second scheme reduces the computational depth from  $O(t^2)$  to  $O(t \log t)$  by using  $t$  auxiliary qubits instead of only 1.

Besides these contributions, we also wrote Python code which effectively implements this compilation technique, demonstrating in practice the promised quantum resource minimization. To the best of our knowledge, this practical demonstration of the usefulness of PBC could not be found in the literature up to this point.

In the context of the considered hidden-shift circuits (HSCs), the resource minimization is clear from the observation of Figures 5 and 6. It is also evident for the larger instances with  $n = t = 42$  compiled by resorting to the dummy simulator as explained in sub-subsection 4.2.3.

In the case of the random quantum circuits (RQCs), the reduction in the number of quantum operations is still relevant (Figure 9), even if the depth of the computation increases with respect to that of the original computation for  $t > 7$ . At this point, it is also worth noting that whenever the original computation is augmented only by Clifford operations, then the quantum resources required for the compiled computation (number of qubits, depth and gate counts) will remain essentially unchanged. As such, in the context of the RQCs considered, if we increased the number of cycles in the input circuits ( $N_{cycles} > 40$ ), we would still have the same results for the compiled computations, even though the original circuits

would now be deeper and have even more single- and two-qubit unitaries. Put differently, our code becomes increasingly advantageous as the ratio  $N_{cycles}/t$  increases.

Moreover, this indifference of the PBC-compilation technique to the addition of extra Clifford gates means that such operations can be regarded essentially as free, similarly to what happens in the one-way model of measurement-based quantum computation. Therefore, these models look very promising for the implementation of techniques or procedures wherein extra Clifford gates are applied in order to realize a given task. A straightforward example is the *classical shadows* technique described in [38]. Succinctly, this technique requires a number of copies of a certain (unknown) quantum state that scales as  $O(\log M)$ , in order to estimate  $M$  properties of that state. The procedure relies on the application of Clifford unitaries, drawn randomly from a certain ensemble, to the unknown quantum state, before measuring it. These extra Clifford unitaries will only change the structure of the PBC to be computed, not the (overall) required resources like the number of qubits or the (average) depth and gate counts.

Finally, our work with hybrid PBC shows how we can extend the number of qubits of the quantum hardware by using a classical (super)computer to simulate  $k$  virtual qubits, at the expense of having a cost exponential in  $k$ . By resorting to a small QPU, this set-up is asymptotically advantageous over the use of the best full classical stabilizer-rank simulators whenever the number qubits traded out is such that  $k \lesssim t/4$ . On the other hand, the use of quantum hardware inevitably implies the presence of coherent and incoherent noise, of which a full classical simulation is otherwise devoid.

There are several natural ways in which this work can be extended and improved, and thus be made even more useful. Firstly, we could adapt the code to allow adaptive Clifford+ $T$  input quantum circuits. This would largely improve our results for the HSCs as we would be able to apply the same adaptive decomposition of the Toffoli gate as used in [22] and [23], effectively reducing the  $T$ -count of each input circuit. In fact, and more interestingly, this advantage will extend to general circuits, as allowing adaptivity will enable the same computation to be encoded

with a smaller number of  $T$  gates, which is the factor that ultimately determines the depth and gate counts of the PBC-compiled circuits.

Secondly, we could explore different pre-compilation techniques, which could be applied to the quantum circuit before running our code. In the context of strong simulation and hybrid PBC, a possibility might be to combine our code with the techniques developed in [26], which sometimes allow for the cancellation of the non-Clifford phases in the  $ZX$ -diagrams.

Another potential line of research that might be worth pursuing relates to the presence of noise in real quantum hardware (briefly touched upon above). The hybrid set-up provides not only a reduction of the number of qubits needed in the actual QPU, but it also guarantees that the virtual qubits are noise-free. In our current hybrid implementation, the code always removes the upper qubits; when thinking about noisy implementations, researching how the choice of different virtual qubits might improve the results in practice might prove significantly beneficial.

Additionally, finding decompositions of  $|A\rangle\langle A|^{\otimes k}$  with less than  $3^k$  terms would have an immediate impact on the cost of performing hybrid PBC. Such decompositions are commonly studied in literature pertaining to the robustness of magic [39, 40] wherein one tries to minimize the  $\ell_1$ -norm of the stabilizer pseudomixture. In our case, the problem translates instead to minimizing the  $\ell_0$ -norm. This might explain why better decompositions are absent from the literature as such optimization problem cannot be solved in polynomial time and, indeed, cannot even be approximated within a constant factor unless  $P = NP$  [41]. Still, we conjecture that better decompositions do exist and, if found, the impact in the cost of hybrid PBC would be extremely relevant.

Finally, on a more engineering-related approach, changing this to a C++ or Julia implementation should reduce the classical processing time, lessening the demands on the coherence of the quantum hardware.

## 6 Acknowledgements

FCRP would like to thank Professor JMB Lopes dos Santos for fruitful discussions and Professor JM Viana P Lopes for providing access to the re-

mote server wherein the code was run. FCRP is supported by the Portuguese institution FCT – Fundação para a Ciência e a Tecnologia via the PhD Research Scholarship 2020.07245.BD. EFG acknowledges funding of the Portuguese institution FCT – Fundação para a Ciência e a Tecnologia via project CEECINST/00062/2018. This work was supported by the H2020-FETOPEN Grant PHOQUSING (GA no.: 899544).

## References

- [1] Peter W. Shor. “Algorithms for quantum computation: discrete logarithms and factoring”. In: *Proceedings 35th Annual Symposium on Foundations of Computer Science*. IEEE Press, Los Alamitos, CA, 1994, pp. 124–134. DOI: [10.1109/SFCS.1994.365700](https://doi.org/10.1109/SFCS.1994.365700).
- [2] Seth Lloyd. “Universal Quantum Simulators”. In: *Science* 273 (1996), pp. 1073–1078. DOI: [10.1126/science.273.5278.1073](https://doi.org/10.1126/science.273.5278.1073).
- [3] Aram W. Harrow, Avinatan Hassidim, and Seth Lloyd. “Quantum Algorithm for Linear Systems of Equations”. In: *Phys. Rev. Lett.* 103 (2009), p. 150502. DOI: [10.1103/PhysRevLett.103.150502](https://doi.org/10.1103/PhysRevLett.103.150502). eprint: <https://arxiv.org/abs/0811.3171v3>.
- [4] Ashley Montanaro. “Quantum algorithms: an overview”. In: *npj Quantum Information* 2 (2016), p. 15023. DOI: [10.1038/npjqi.2015.23](https://doi.org/10.1038/npjqi.2015.23). eprint: <https://arxiv.org/abs/1511.04206v2>.
- [5] John Preskill. “Quantum Computing in the NISQ era and beyond”. In: *Quantum* 2 (2018), p. 79. DOI: [10.22331/q-2018-08-06-79](https://doi.org/10.22331/q-2018-08-06-79).
- [6] Frank Arute et al. “Quantum supremacy using a programmable superconducting processor”. In: *Nature* 574 (2019), pp. 505–510. DOI: [10.1038/s41586-019-1666-5](https://doi.org/10.1038/s41586-019-1666-5).
- [7] Han-Sen Zhong et al. “Quantum computational advantage using photons”. In: *Science* 370 (2020), pp. 1460–1463. DOI: [10.1126/science.abe8770](https://doi.org/10.1126/science.abe8770). eprint: <https://arxiv.org/abs/2012.01625>.

- [8] Yulin Wu et al. “Strong Quantum Computational Advantage Using a Superconducting Quantum Processor”. In: *Phys. Rev. Lett.* 127 (2021), p. 180501. DOI: [10.1103/PhysRevLett.127.180501](https://arxiv.org/abs/2106.14734). eprint: <https://arxiv.org/abs/2106.14734>.
- [9] Alberto Peruzzo et al. “A variational eigenvalue solver on a photonic quantum processor”. In: *Nature Communications* 5 (2014), p. 4213. DOI: [10.1038/ncomms5213](https://arxiv.org/abs/1304.4801).
- [10] Vedran Dunjko, Yimin Ge, and J. Ignacio Cirac. “Computational Speedups Using Small Quantum Devices”. In: *Phys. Rev. Lett.* 121 (2018), p. 250501. DOI: [10.1103/PhysRevLett.121.250501](https://arxiv.org/abs/1807.08970v2). eprint: <https://arxiv.org/abs/1807.08970v2>.
- [11] Aram W. Harrow. *Small quantum computers and large classical data sets*. 2020. eprint: <https://arxiv.org/abs/2004.00026>.
- [12] Sergey Bravyi, Graeme Smith, and John A. Smolin. “Trading Classical and Quantum Computational Resources”. In: *Phys. Rev. X* 6 (2016), p. 021043. DOI: [10.1103/PhysRevX.6.021043](https://arxiv.org/abs/1506.01396). eprint: <https://arxiv.org/abs/1506.01396>.
- [13] Mithuna Yoganathan, Richard Jozsa, and Sergii Strelchuk. “Quantum advantage of unitary Clifford circuits with magic state inputs”. In: *Proc. R. Soc. A* 475 (2019), p. 20180427. DOI: [10.1098/rspa.2018.0427](https://arxiv.org/abs/1804.0427).
- [14] Padraic Calpin. “Exploring Quantum Computation Through the Lens of Classical Simulation”. PhD thesis. UCL (University College London), 2020. URL: <https://discovery.ucl.ac.uk/id/eprint/10091573>.
- [15] Daniel Gottesman. “Stabilizer Codes and Quantum Error Correction”. PhD thesis. Caltech, 1997. eprint: <https://arxiv.org/abs/quant-ph/9705052>.
- [16] Daniel Gottesman. “The Heisenberg Representation of Quantum Computers”. In: *Group22: Proceedings of the XXII International Colloquium on Group Theoretical Methods in Physics*. 1998. eprint: <https://arxiv.org/abs/quant-ph/9807006>.
- [17] Igor L. Markov and Yaoyun Shi. “Simulating Quantum Computation by Contracting Tensor Networks”. In: *SIAM Journal on Computing* 38 (2008), pp. 963–981. DOI: [10.1137/050644756](https://arxiv.org/abs/quant-ph/0511069v7). eprint: <https://arxiv.org/abs/quant-ph/0511069v7>.
- [18] Cupjin Huang, Michael Newman, and Mario Szegedy. *Explicit lower bounds on strong quantum simulation*. 2018. eprint: <https://arxiv.org/abs/1804.10368v2>.
- [19] Hakop Pashayan, Joel J. Wallman, and Stephen D. Bartlett. “Estimating Outcome Probabilities of Quantum Circuits Using Quasiprobabilities”. In: *Phys. Rev. Lett.* 115 (2015), p. 070501. DOI: [10.1103/PhysRevLett.115.070501](https://arxiv.org/abs/1503.07525v2). eprint: <https://arxiv.org/abs/1503.07525v2>.
- [20] Robert Raussendorf et al. “Phase-space-simulation method for quantum computation with magic states on qubits”. In: *Phys. Rev. A* 101 (2020), p. 012350. DOI: [10.1103/PhysRevA.101.012350](https://arxiv.org/abs/1905.05374v3). eprint: <https://arxiv.org/abs/1905.05374v3>.
- [21] Scott Aaronson and Daniel Gottesman. “Improved simulation of stabilizer circuits”. In: *Phys. Rev. A* 70 (2004), p. 052328. DOI: [10.1103/PhysRevA.70.052328](https://arxiv.org/abs/quant-ph/0406196v5). eprint: <https://arxiv.org/abs/quant-ph/0406196v5>.
- [22] Sergey Bravyi and David Gosset. “Improved Classical Simulation of Quantum Circuits Dominated by Clifford Gates”. In: *Phys. Rev. Lett.* 116 (2016), p. 250501. DOI: [10.1103/PhysRevLett.116.250501](https://arxiv.org/abs/1601.07601v3). eprint: <https://arxiv.org/abs/1601.07601v3>.
- [23] Sergey Bravyi et al. “Simulation of quantum circuits by low-rank stabilizer decompositions”. In: *Quantum* 3 (2019), p. 181. DOI: [10.22331/q-2019-09-02-181](https://arxiv.org/abs/2019-09-02-181).
- [24] Hammam Qassim, Joel J. Wallman, and Joseph Emerson. “Clifford recompilation for faster classical simulation of quantum circuits”. In: *Quantum* 3 (2019), p. 170. DOI: [10.22331/q-2019-08-05-170](https://arxiv.org/abs/2019-08-05-170).
- [25] Hammam Qassim, Hakop Pashayan, and David Gosset. “Improved upper bounds on the stabilizer rank of magic states”. In: *Quantum* 5 (2021), p. 606. DOI: [10.22331/q-2021-12-20-606](https://arxiv.org/abs/2021-12-20-606).

- [26] Aleks Kissinger and John van de Wetering. *Simulating quantum circuits with ZX-calculus reduced stabiliser decompositions*. 2021. eprint: <https://arxiv.org/abs/2109.01076>.
- [27] Xinlan Zhou, Debbie W. Leung, and Isaac L. Chuang. “Methodology for quantum logic gate construction”. In: *Phys. Rev. A* 62 (2000), p. 052316. DOI: [10.1103/PhysRevA.62.052316](https://arxiv.org/abs/quant-ph/0002039v2). eprint: <https://arxiv.org/abs/quant-ph/0002039v2>.
- [28] Sergey Bravyi and Alexei Kitaev. “Universal quantum computation with ideal Clifford gates and noisy ancillas”. In: *Phys. Rev. A* 71 (2005), p. 022316. DOI: [10.1103/PhysRevA.71.022316](https://arxiv.org/abs/quant-ph/0403025v2). eprint: <https://arxiv.org/abs/quant-ph/0403025v2>.
- [29] Earl T. Campbell, Barbara M. Terhal, and Christophe Vuillot. “Roads towards fault-tolerant universal quantum computation”. In: *Nature* 549 (2017), pp. 172–179. DOI: [10.1038/nature23460](https://arxiv.org/abs/1612.07330v2). eprint: <https://arxiv.org/abs/1612.07330v2>.
- [30] Daniel Litinski. “Magic State Distillation: Not as Costly as You Think”. In: *Quantum* 3 (2019), p. 205. DOI: [10.22331/q-2019-12-02-205](https://arxiv.org/abs/1912.02233v1).
- [31] Ketan N. Patel, Igor L. Markov, and John P. Hayes. *Efficient Synthesis of Linear Reversible Circuits*. 2003. eprint: <https://arxiv.org/abs/quant-ph/0302002>.
- [32] Diogo Cruz et al. “Efficient Quantum Algorithms for GHZ and W States, and Implementation on the IBM Quantum Computer”. In: *Advanced Quantum Technologies* 2.5-6 (2019), p. 1900015. DOI: <https://doi.org/10.1002/qute.201900015>. eprint: <https://arxiv.org/abs/1807.05572>.
- [33] Jay Gambetta, Ismael Faro, and Karl Wehden. *IBM’s roadmap for building an open quantum software ecosystem*. 2021. URL: <https://research.ibm.com/blog/quantum-development-roadmap> (visited on 10/21/2021).
- [34] Qiskit Development Team. *Statevector Simulator*. 2022. URL: <https://qiskit.org/documentation/stubs/qiskit.providers.aer.StatevectorSimulator.html#> (visited on 11/01/2022).
- [35] Çetin K. Koç and Sarath N. Arachchige. “A fast algorithm for gaussian elimination over GF(2) and its implementation on the GAPP”. In: *Journal of Parallel and Distributed Computing* 13 (1991), pp. 118–122. DOI: [10.1016/0743-7315\(91\)90115-P](https://doi.org/10.1016/0743-7315(91)90115-P).
- [36] Vivek V. Shende and Igor L. Markov. “On the CNOT-cost of TOFFOLI gates”. In: *Quantum Info. Comput.* 9 (2009), pp. 461–486. DOI: [10.26421/QIC8.5-6-8](https://arxiv.org/abs/0803.2316). eprint: <https://arxiv.org/abs/0803.2316>.
- [37] Sergio Boixo et al. “Characterizing quantum supremacy in near-term devices”. In: *Nature Physics* 14 (2018), pp. 595–600. DOI: [10.1038/s41567-018-0124-x](https://arxiv.org/abs/1608.00263v3). eprint: <https://arxiv.org/abs/1608.00263v3>.
- [38] Hsin-Yuan Huang, Richard Kueng, and John Preskill. “Predicting many properties of a quantum system from very few measurements”. In: *Nature Physics* 16 (2020), pp. 1050–1057. DOI: <https://doi.org/10.1038/s41567-020-0932-7>. eprint: <https://arxiv.org/abs/2002.08953v2>.
- [39] Mark Howard and Earl Campbell. “Application of a Resource Theory for Magic States to Fault-Tolerant Quantum Computing”. In: *Phys. Rev. Lett.* 118 (2017). DOI: [10.1103/PhysRevLett.118.090501](https://arxiv.org/abs/1609.07488v2). eprint: <https://arxiv.org/abs/1609.07488v2>.
- [40] Markus Heinrich and David Gross. “Robustness of Magic and Symmetries of the Stabiliser Polytope”. In: *Quantum* 3 (2019), p. 132. DOI: [10.22331/q-2019-04-08-132](https://arxiv.org/abs/1904.08132).
- [41] Edoardo Amaldi and Viggo Kann. “On the approximability of minimizing nonzero variables or unsatisfied relations in linear systems”. In: *Theoretical Computer Science* 209 (1998), pp. 237–260. DOI: [10.1016/S0304-3975\(97\)00115-1](https://doi.org/10.1016/S0304-3975(97)00115-1).